AIMS Mathematics, 11(2): 4147–4199.
DOI:10.3934/math.2026167
Received: 29 October 2025
Revised: 27 January 2026
Accepted: 29 January 2026
Published: 10 February 2026

https://www.aimspress.com/journal/Math

Research article

Mathematical model of Mpox: assessing the impact of early therapeutic education on seasonal variation

Mohammed M Al-Shomrani[1,*] **and Abdullahi Yusuf**[2,3,4,*]

[1] Department of Mathematics, Faculty of Science, King Abdulaziz University, Jeddah 21589, Saudi Arabia

[2] Department of Mathematics, Firat University, Elazig, Turkiye

[3] Department of Mathematics, Saveetha School of Engineering, Saveetha Institute of Medical and Technical Sciences, Saveetha University, Chennai 602105, Tamil Nadu, India

[4] Faculty of Engineering and Natural Sciences, Istanbul Okan University, Istanbul, Turkiye

* **Correspondence:** Email: malshamrani@kau.edu.sa, ayusuf@firat.edu.tr.

Abstract: The 2022–2023 global monkeypox (Mpox) virus outbreak, which affected more than 100 nations, has highlighted the importance of effective public health measures and predictive modeling techniques. In this work, we formulated a mathematical model (MD) of Mpox to assess the impact of early therapeutic education on seasonal variation. To guarantee epidemiological viability, we demonstrated the boundedness and positivity of the model. The next-generation matrix method was employed to determine the basic reproduction number and evaluate the stability of the disease-free equilibrium at the local and global levels. We assessed the existence of an arbitrary equilibrium. The center manifold theorem was employed to assess the backward bifurcation, which shows that imperfect vaccination causes the backward bifurcation. An evaluation of the existence of an endemic equilibrium point was also conducted. The global stability of an endemic equilibrium point was established through the application of a nonlinear Lyapunov function of the Goh-Voltterra type. Data fitting was done to show the model's fitness and estimate the data's parameters. Sensitivity analysis was ascertained. Seasonal variation was assessed. In a numerical simulation, we assessed five controls, which indicated that early therapeutic education is the most effective way to control the re-emergence of Mpox disease in the human (HUM) population.

Keywords: mathematical model; monkeypox; parameter estimation; therapeutic; education; seasonal Variation
Mathematics Subject Classification: 26A33, 34A08, 34A34, 65L20, 92D30

1. Introduction

The world was plagued by the deadly COVID-19 virus (SARS-CoV-2) for more than two years. Mpox, another known zoonotic viral disease, gained attention before the end of this pandemic and resulted in a notable number of cases in 2022 [1]. Many nations are currently dealing with several epidemics, each brought on by a distinct kind of newly emerging or reemerging virus. Since the World Health Organization (WHO) recently announced a recurrence of the MPOX outbreak, with the disease reemerging and spreading across numerous nations worldwide, Mpox sickness is one of these urgent circumstances that requires proper monitoring [2]. The zoonotic viral disease known as Mpox is brought on by the Mpox virus, a member of the Orthopoxvirus genus in the Poxviridae family. The virus was first discovered in Danish captive monkeys in 1958, and it was discovered in people in the Democratic Republic of the Congo (DRC) in 1970 [3, 4]. Mpox, which has historically only been found in Central and West Africa, has recently attracted international attention because of large outbreaks in non-endemic areas. Over the past several years, there has been a noticeable change in the epidemiology of Mpox. In May 2022, the WHO documented a multi-country outbreak, revealing patients in previously unknown nations. Because of this, Mpox was designated a public health emergency of international concern (PHEIC) by the WHO in July 2022 [4,5]. More than 92,000 confirmed cases and 171 fatalities had been reported in 116 countries by December 2023, [6,7]. Mpox can spread from person to person as well as from animal to HUM. Rodents and primates are possible reservoirs for animal-to-HUM transmission, which can occur through direct contact with the blood, body fluids, or lesions of infected animals [3, 4]. The main ways that HUMs can spread the disease to one another are by respiratory droplets from extended in-person contact, direct touch with infectious skin lesions, or contact with contaminated clothing or bedding [8]. Interestingly, the 2022 outbreak brought to light how intimate contact contributes to the transmission inside men who have sex with men (MSM) communities [8].

Furthermore, the incubation period lasts seven to fourteen days [9]. The illness lasts for 2–4 weeks, and the patient develops elevated bumps 1–3 days after the fever starts [10]. Consequently, the reported case fatality ratio ranges from 1% to 10% [10]. Research from Africa indicates that those who had received the smallpox vaccine had a lower risk of developing Mpox, even though there are presently no vaccines to prevent Mpox [11]. The Centers for Disease Control and Prevention recommended the smallpox vaccine for anyone involved in epidemic investigations and for those providing care to afflicted individuals to protect against Mpox [11]. For up to 14 days after exposure, vaccination is recommended for people who have been exposed [11]. Clinically, Mpox shares symptoms with smallpox; however, it usually progresses more mildly. After an incubation period of five to twenty-one days, there occurs a prodromal phase that is distinguished from smallpox by fever, headache, myalgia, and lymphadenopathy [12]. Following this, a centrifugal rash appears, progressing through macular, papular, vesicular, and pustular phases before crusting over and resolving in 2 to 4 weeks. Although severe cases are rare, they can happen, particularly in pregnant women, children, and those with weakened immune systems [12]. Regarding early therapeutic education and seasonal variation, [13] formulated a mathematical model of Onchocerciasis transmission dynamics through incorporating early therapeutic intervention and vector control, by introducing a mathematical model integrating early treatment of exposed individuals as an intervention to arrest the disease at the microfilariae stage and halt its progression to the macrofilariae stage. The model focuses on the impact of early

treatment, vector control, and infectious treatment rates in mitigating transmission. [14] formulated a mathematical model for Onchocerciasis transmission dynamics, which effectively captured early treatment and vector management strategies.

Understanding the epidemiology of Mpox is challenging because it has not received much attention in the past. Nevertheless, a variety of MDs have been created recently to examine the dynamics of Mpox. For the Mpox outbreak, a new MD based on a deterministic method was created and studied in [15]. According to their research, separating affected individuals from other groups lowers the incidence of disease. The existence and uniqueness of solutions are established using the Picard–Lindelöf technique, guaranteeing the mathematical soundness of the model. In [1], an analysis and presentation of a modified logistic growth model was provided. They primarily concentrated on two non-pharmaceutical interventions: laws designed to lessen transmission from one person to another and from animals to HUMs. To determine their short-term impact on epidemics and assess their efficacy in reducing infected cases, they included these two tactics as control parameters in the model. According to their research, ongoing use of preventative measures may be a useful strategy to stop a brief outbreak of Mpox or related illnesses. In [2], they used a deterministic MD within a constant proportional-Caputo derivative framework to conduct a thorough analysis of the Mpox virus. Their research showed that the variables in their situation could be included in the processes that regulate the spread of Mpox.

[16] established a mathematical assessment of Mpox disease with the impact of vaccination. Their model formulation took into account the HUM population's poor immunization. Their simulation results provide a pictorial representation of the impact of disease occurrence. In [17], their study examines many epidemiological facets of Mpox virus infection. Their objective was to assess how vaccination and therapy affected the dynamics of viral transmission. To integrate faulty vaccination and treatment as control measures within the HUM population, the model first uses integer-order nonlinear differential equations. In [18], they formulated a brand-new MD that incorporates both direct and indirect transmission pathways, as well as the impacts of vaccination, to represent the dynamics of Mpox transmission between HUM and rodent populations. Their findings highlight how improving recovery rates and expanding immunization coverage can greatly lower the burden of disease. In [19], they examine a hybrid forecasting system that was developed for new cases and death counts for MPV infection using the world daily cumulative confirmed and death series. [20] introduced a novel model that simulates the spread of the monkeypox virus [21]. Their new model takes into account the effect of the interaction between the human and rodent population, along with some realistic factors that have not been introduced before, such as imperfect vaccination and nonlinear incidence rates. Moreover, they further subdivide the HUM population into low-risk and high-risk groups to better reflect recent observations. Their new findings aimed at developing preventive control measures to suppress the spread of the virus and to develop effective strategies for controlling and preventing outbreaks, ultimately protecting public health and minimizing the impact of the disease.

Considering all the above-reviewed articles, one can easily see that some of the MDs used fractional-order derivative, imperfect vaccination, direct and indirect transmission to study Mpox dynamics, but none of the above considered early therapeutic education and seasonal variation. This work formulated a deterministic model to study Mpox, which took early therapeutic education, imperfect vaccination, education, post-exposure vaccination, and seasonal variation. We specifically targeted the impact of early therapeutic education on the proposed model to study. Also, seasonal changes can indirectly

affect human immunity (due to other circulating pathogens or nutritional factors) and human behaviors (e.g., more indoor contact in some seasons), which might influence susceptibility and transmission rates [22–24]. We were able to achieve the following points:

- A brand new MD of Mpox: assessing the impact of early therapeutic education on seasonal variation.
- Existence of solutions and their boundedness was ascertained.
- Boundedness and positivity of solutions were ascertained.
- Existence of an arbitrary equilibrium was ascertained.
- Reproduction number was calculated using the spectral radius.
- Local stability of the disease-free equilibrium was ascertained.
- Backward bifurcation analysis was ascertained.
- Global stability of the disease-free equilibrium was ascertained.
- Existence endemic equilibrium point was ascertained.
- Global stability of the endemic equilibrium point was ascertained.
- Uncertainty and sensitivity analysis of the model parameters Latin hypercube sampling and partial rank correction coefficient was ascertained.
- Models were validated and parameter values were accurately determined via data fitting.
- Impact of early therapeutic education was ascertained.
- Seasonal variation analysis was ascertained.

The research is organized as follows: Section 1 captures the introductory parts; Section 2 captures model building and assumptions; Section 3 captures the analytical analysis of the model; Section 4 captures the data fittings of the model; Section 5 captures the numerical simulation part of the model, the discussions of the simulated figures, and seasonal dynamics simulation of the model; and Section 6 gives the conclusion and recommendations of the study.

2. Model description

A viral condition called Mpox can result in a painful rash, swollen lymph nodes, fever, headache, back discomfort, muscular aches, and low energy [25]. Some patients become quite ill, but most people recover completely. This disease has the potential to be transmitted between HUMs, from rodent to rodent, and from rodents to HUMs. We consider the populations of the HUM and rodent. The population of HUM are partitioned into five (5) compartments, while that of rodent into three (3). The HUM compartments are: susceptible HUMs (S_h), exposed HUMs (E_h), vaccinated HUMs (V_h), infectious HUMs (I_h), and removed HUMs. The rodent populations are: susceptible rodents (S_r), exposed rodents (E_r), and infectious rodents (I_r). The susceptible HUM (S_h) is generated at rate Φ_h, which is the rate at which HUMs are recruited into the population, that is, the HUM total population (M_h), which further increases due to the waning of imperfect vaccination at the rate (ϑ). The compartment decreases due to the exposure of susceptible HUMs to infectious HUMs and infectious rodents at the rate $\phi_h = \frac{(1-\chi)\varrho_h(I_h+\alpha I_r)}{M_h}$, where χ is the education rate, ϱ_h is the contact effectiveness rate of HUMs, α is the parameter of modification due to reduced contact of HUMs with rodents; the compartment further decreases due to imperfect vaccination at the rate ϖ. The exposed HUMs (E_h) are generated due to the exposure of susceptible HUMs to infectious HUMs and infectious rodents at

the rate $\phi_h = \frac{(1-\chi)\varrho_h(I_h+\alpha I_r)}{M_h}$, where χ is the education rate, ϱ_h is the contact effectiveness rate of HUMs, α is the parameter of modification due to reduced contact of HUMs with rodents. The compartment decreases due to early therapeutic education (ψ), that is, frequent check-ups need to be done in the concerned population (this means that with frequent check-ups, one can detect the disease an early stage and this will enable the health workers to treat it early to reduce the transmission in the in society) at the rate $p_h\psi$, where p_h is the rate of progression. Others progresses to become infectious HUMs at the rate $p_h(1-\chi)$ and they further reduces at μ, which is the post-exposure vaccination rate to the vaccinated compartment.

The vaccinated HUM (V_h) is generated due to post-exposure vaccination and imperfect vaccination, that is μ and ϖ, respectively. The compartment is diminished at the rates ϑ and γ, which are the waning rate of imperfect vaccination and the rate at which the vaccinated compartment incurs permanent immunity, respectively. The infectious HUM (I_h) arises from the advancement of the exposed HUMs at the rate $p_h(1-\chi)$. The compartment reduces due to Mpox mortality and treatment, leading to permanent immunity at rates δ_h and τ, respectively. The removed HUM (R_h) is generated by early therapeutic education (ψ) at the rate $p_h\psi$, where p_h is the progression rate, which also increases due to the treatment rate, leading to permanent immunity at the rate τ. Additionally, it increases further due to the rate at which the vaccinated compartment acquires permanent immunity (γ). All the HUM compartments are reduced due to the HUM natural mortality rate (υ_h).

The susceptible rodent (S_r) is generated at rate Φ_r, which is the rate at which rodents are recruited into the population, that is, the rodent total population (M_r). The compartment decreases due to the exposure of susceptible rodents to infectious rodents at the rate $\phi_r = \frac{\varrho_r I_r}{M_r}$, where ϱ_r is the contact effectiveness rate of rodents. The exposed rodents (E_r) increase due to the exposure of susceptible rodents to infectious rodents at the rate $\phi_r = \frac{\varrho_r I_r}{M_r}$, where ϱ_r is the contact effectiveness rate of rodents. The compartment diminishes as a result of the progression rate (p_r). The infectious rodent arises from the progression (p_r) of the exposed rodent. All the rodent compartments are reduced due to the rodent natural mortality rate (υ_r).

2.1. Model assumption

The following are assumptions considered during the formulation of model (2.1):

- It is assumed that the immunity of some of those who are vaccinated can wane, while others can get permanent immunity.
- It is assumed that HUMs can get the disease from rodents, but rodents cannot get it from HUMs (this is necessary because HUMs tend to hunt most of the rodents they come across). The fact that humans eat rodents makes it almost impossible for humans to get in contact with a rodent without killing it, but the reverse is not true. Although, this is a model limitation.
- It is assumed that there is a homogeneous mixture of population in the HUM population.

2.2. Principal challenges of the problem under consideration

First, because infected people frequently show no symptoms or only mild ones during the early exposure period, Mpox demonstrates delayed detection and underreporting. This delay maintains transmission chains by enabling undiscovered patients to advance into the infectious stage. Therefore, traditional management methods that mainly concentrate on treating symptomatic individuals take

action too late to successfully inhibit transmission. Second, there is uncertainty regarding long-term disease control due to inadequate vaccination and declining immunity. Over time, vaccinated people may still become vulnerable, which could result in recurring outbreaks and undermine the use of vaccination as a stand-alone intervention. Third, controlling outbreaks is made more difficult by seasonal variations in the strength of transmission. Static or time-invariant intervention measures are insufficient since human behavior, movement, and contact patterns might fluctuate and increase transmission during specific periods.

Fourth, there are other ways that Mpox might spread, including encounters between humans and rodents. This zoonotic element makes the system more complex and reduces the efficacy of interventions that focus on a single population or mode of transmission. Lastly, budget limitations prevent widespread testing, large-scale treatment programs, and quick vaccination deployment in many settings, especially in low- and middle-income areas. This calls for alternative, more affordable control strategies.

2.3. Resolution using the suggested modeling and control framework

These difficulties are addressed by the suggested mathematical model, which specifically includes early therapeutic education as a control mechanism operating at the exposed stage. By facilitating early case identification, fast isolation, and timely healthcare interaction, this strategy helps to avoid the infectious stage. The model shows a substantial decrease in the overall illness burden by stopping transmission before peak infectiousness. Because waning immunity and imperfect vaccination are clearly described, the framework can accurately depict recurrent transmission dynamics and evaluate the drawbacks of vaccine-only approaches. This makes it possible for policymakers to comprehend the circumstances in which more controls must be added to vaccination. Time-dependent transmission rates are used to account for seasonal variance, guaranteeing that the model accounts for sporadic increases in the risk of infection. This shows that early therapeutic education is still beneficial even during high-transmission seasons and enables assessment of intervention robustness under changing epidemiological settings.

The zoonotic nature of Mpox transmission is addressed by including both human and rodent populations, giving a more complete picture of disease dynamics. Assessing human-focused treatments without ignoring the impact of animal reservoirs is made possible by this integrated system. Lastly, the model-based comparison of various control techniques offers quantitative proof that early therapeutic education is not only cost-effective and operationally possible, but also epidemiologically effective, especially in settings with limited resources. Thus, by fusing mathematical rigor with public health relevance, the suggested system provides a workable solution to the mentioned challenges.

Figure 1 illustrates the schematic representation of Mpox based on the aforementioned assumptions, while model (2.1) presents the pertinent model equations derived from Figure 1. The interpretations of the variables and parameters are presented in Tables 1 and 2, respectively.

$$
\begin{aligned}
\frac{dS_h}{dt} &= \Phi_h + \vartheta V_h - \phi_h S_h - (\upsilon_h + \varpi) S_h, \\
\frac{dE_h}{dt} &= \phi_h S_h - (p_h + \upsilon_h + \mu) E_h, \\
\frac{dV_h}{dt} &= \varpi S_h + \mu E_h - (\vartheta + \upsilon_h + \gamma) V_h, \\
\frac{dI_h}{dt} &= p_h(1-\psi) E_h - (\upsilon_h + \delta_h + \tau) I_h, \\
\frac{dR_h}{dt} &= \tau I_h + \gamma V_h + p_h \psi E_h - \upsilon_h R_h, \\
\frac{dS_r}{dt} &= \Phi_r - \phi_r S_r - \upsilon_r S_r, \\
\frac{dE_r}{dt} &= \phi_r S_r - (p_r + \upsilon_r) E_r, \\
\frac{dI_r}{dt} &= p_r E_r - \upsilon_r I_r,
\end{aligned}
\tag{2.1}
$$

where

$$
\begin{aligned}
\phi_h &= \frac{(1-\chi)\varrho_h (I_h + \alpha I_r)}{M_h}, \\
\phi_r &= \frac{\varrho_r I_r}{M_r}.
\end{aligned}
\tag{2.2}
$$

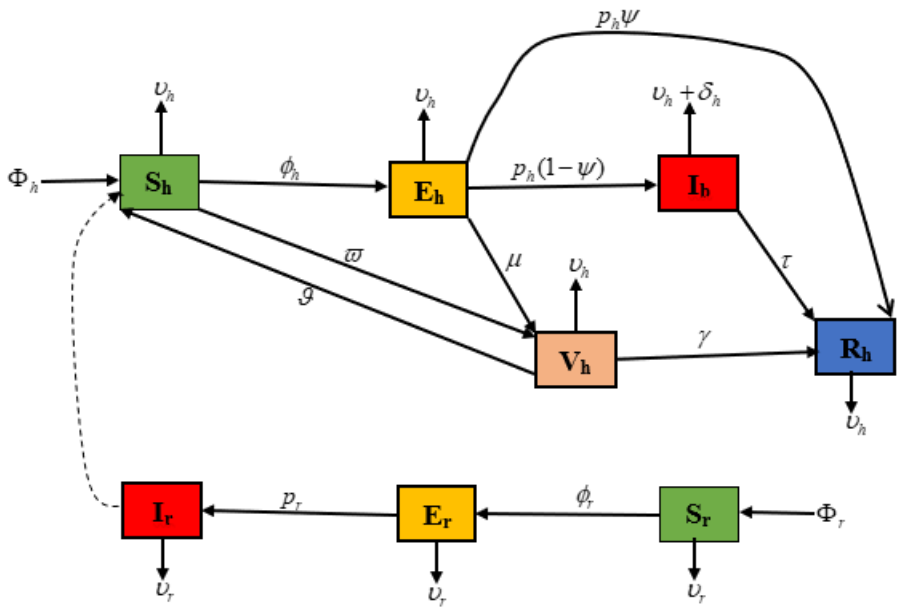

Figure 1. Schematized diagram of Mpox.

Table 1. State variables interpretation used in the formulation of model (2.1).

State variable	Interpretation
S_h	Susceptible HUMs
E_h	Exposed HUMs
V_h	Vaccinated HUMs
I_h	Infectious HUMs
R_h	Removed HUMs
S_h	Susceptible rodents
V_h	Vaccinated rodents
I_r	Infectious rodents
M_h, M_r	Total population of HUMs, and rodents

Table 2. Parameters used in the formulation of model (2.1).

Parameter	Range	Reference	Interpretation
Φ_h, Φ_r	10000,50000	[26, 27]	HUMs, and rodents recruitment rates
υ_h, υ_r	0.0014,0.01042	[26, 28]	HUM, and rodents natural mortality rate
χ	0.000001	fitted	Education rate
ϱ_h, ϱ_r	0.5,0.83	[29, 30]	Contact effectiveness rates of HUMs, and rodents
α	0.05	[29, 30]	Parameter of modification due to reduced contact of HUMs with rodents
p_h, p_r	0.089,0.0712	[29, 30]	Progression rates of HUMs and rodents
ϖ	0.579718	fitted	Imperfect-vaccination rate
δ_h	0.17	[29, 30]	Disease-induced death rate of infectious HUMs
ϑ	0.000001	fitted	Vaccine waning rate of HUMs
μ	(0,1)	variable	post-exposure vaccination rate
γ	0.081	[29, 30]	Immunity rate
τ	0.000001	fitted	treatment rate
ψ	0.408492	fitted	Early therapeutic education

3. Fundamental characteristics of the model

The computation of the basic reproduction number, positivity and boundedness of solutions, and all of the classical analysis of model (2.1) are covered in this section.

3.1. Existence, boundedness and positivity of solutions, and their uniqueness

To ascertain whether a solution to the model (2.1) exists, a rigorous test will be conducted to confirm its uniqueness. Its uniqueness must be proven if it is confirmed. It is determined using the Lipschitz

criteria in this way:

$$\begin{aligned}
\Lambda_1 &= \Phi_h + \vartheta V_h - \left(\frac{(1-\chi)\varrho_h(I_h+\alpha I_r)}{M_h} + \upsilon_h + \varpi\right)S_h,\\
\Lambda_2 &= \frac{(1-\chi)\varrho_h(I_h+\alpha I_r)}{M_h}S_h - (p_h+\upsilon_h+\mu)\,E_h,\\
\Lambda_3 &= \varpi S_h + \mu S_h - (\vartheta+\upsilon_h+\gamma)V_h,\\
\Lambda_4 &= p_h(1-\psi)E_h - (\upsilon_h+\delta_h+\tau)I_h,\\
\Lambda_5 &= \tau I_h + \gamma V_h + p_h\psi E_h - \upsilon_h R_h,\\
\Lambda_6 &= \Phi_r - \frac{\varrho_r I_r}{M_r}S_r - \upsilon_r S_r,\\
\Lambda_7 &= \frac{\varrho_r I_r}{M_r}S_r - (\upsilon_r+p_r)E_r,\\
\Lambda_8 &= p_r E_r - \upsilon_r I_r.
\end{aligned} \tag{3.1}$$

In the domain $0 \le \mathrm{B} \le \mathrm{G}$ where the partial derivative is within $\delta_t \le \mathrm{B} \le \mathrm{G}$, where δ_t and G are constants bigger than zero, the boundedness of the solution of model (2.1) will be examined.

Theorem 3.1. *In the region* $0 \le \mathrm{B} \le \mathrm{G}$ *in* $\mathcal{D}$*, the model* (2.1) *has a unique solution, given that*

$$\frac{d\Lambda_i}{dt_j}, i, j = 1, 2, \ldots 8 \tag{3.2}$$

in $0 \le \mathrm{B} \le \mathrm{G}$ is bounded and continuous.

Proof. By partially differentiating Λ_1 in relation to each state variable in (2.1), we obtain

$$\begin{aligned}
\left|\frac{\partial\Lambda_1}{\partial S_h}\right| &= \left|-\left(\frac{(1-\chi)\varrho_h(I_h+\alpha I_r)}{M_h} + \upsilon_h + \varpi\right)\right| < \infty,\\
\left|\frac{\partial\Lambda_1}{\partial E_h}\right| &= \left|\frac{\partial\Lambda_1}{\partial V_h}\right| = \left|\frac{\partial\Lambda_1}{\partial R_h}\right| = \left|\frac{\partial\Lambda_1}{\partial S_r}\right| = \left|\frac{\partial\Lambda_1}{\partial E_r}\right| = 0 < \infty,\\
\left|\frac{\partial\Lambda_1}{\partial I_h}\right| &= \left|-\frac{(1-\chi)\varrho_h}{M_h}\right| < \infty,\\
\left|\frac{\partial\Lambda_1}{\partial I_r}\right| &= \left|-\frac{(1-\chi)\varrho_h\alpha}{M_h}\right| < \infty.
\end{aligned} \tag{3.3}$$

For $\Lambda_2, \Lambda_3, \Lambda_4, \Lambda_5, \Lambda_6, \Lambda_7,$, and Λ_8, the same procedure may be carried out. As a result, model (2.1) exists and has a unique solution in $\mathcal{D}$ since all the partial derivatives are smaller than infinity. □

3.2. Solutions' boundedness and positivity

We demonstrate the boundedness and positivity of the system (2.1) in this subsection. For the model (2.1) specified by Λ, let $\mathcal{D}$ be a good physiologically viable region.
Let

$$\mathcal{D} = \mathcal{D}_h \times \mathcal{D}_r, \tag{3.4}$$

$$\mathcal{D}_h = \{(S_h, E_h, V_h, I_h, R_h) \in R_+^5 : M_h \le \frac{\Phi_h}{\upsilon_h}\}, \tag{3.5}$$

and

$$\mathcal{D}_r = \{(S_r, E_r, I_r) \in R_+^3 : M_r \leq \frac{\Phi_r}{\upsilon_r}\}, \tag{3.6}$$

Theorem 3.2. *Assume that the model's initial values are as follows:* $\{(S_h(0), E_h(0), V_h(0), I_h(0), R_h(0), S_r(0), E_r(0), I_r(0)) \geq 0\} \in \mathcal{D}$. *After that, the set of solutions* $\{S_h(t), E_h(t), V_h(t), I_h(t), R_h(t), S_r(t), E_r(t), I_r(t)\}$ *of model* (2.1)*, is positive for all* $t > 0$.

Proof. We must demonstrate that the variables in the solution $(S_h(t), E_h(t), V_h(t), I_h(t), R_h(t), S_r(t), E_r(t), I_r(t))$ of model (2.1) according to the initial conditions on the basis of $S_h(0) > 0, E_h(0) > 0, V_h(0) > 0, I_h(0) > 0, R_h(0) > 0, S_r(0) > 0, E_r(0) > 0$, and $I_r(0) > 0$, are non-negative.

Let $t_1 = sup(t > 0|\forall \Lambda \in [0, 1], S_h(\Lambda) > 0, E_h(\Lambda), V_h(\Lambda) > 0, I_h(\Lambda) > 0, R_h(\Lambda) > 0, S_r(\Lambda) > 0, E_r(\Lambda) > 0, I_r(\Lambda) > 0)$. The existence of t_1 is guaranteed by the aforementioned initial conditions in addition to the continuity of all functions $S_h, E_h, V_h, I_h, R_h, S_r, E_r$, and I_r. All of the model (2.1) solutions are positive if $t_1 = \infty$. At least one solution $S_h(t), E_h(t), V_h(t), I_h(t), R_h(t), S_r(t), E_r(t), I_r(t)$ equals zero at value t_1 if $t_1 < \infty$, i.e., t_1 is finite, by definition, (since t_1 is a supremum).

Let us assume that $S(t_1) = 0$, and let's look at model (2.1)'s first equation:

$$\frac{dS_h(t)}{dt} = \Phi_h + \vartheta V_h - (\phi_h + \upsilon_h + \varpi) S_h(t). \tag{3.7}$$

For every $t \in [0, t_1]$, we know that $\Phi_h + \vartheta V_h \geq 0$. Consequently,

$$\frac{dS_h(t)}{dt} + (\phi_h + \upsilon_h + \varpi) S_h(t) \geq 0. \tag{3.8}$$

Hence,

$$\begin{aligned}
&\frac{d}{dt}\left[S_h(t) exp\left(\int_0^t \phi_h(\tau)d\tau + (\upsilon_h + \varpi)t\right)\right] \\
&= \frac{dS_h(t)}{dt} exp\left(\int_0^t \phi_h(\tau)d\tau + (\upsilon_h + \varpi)t\right) \\
&+ S_h(t)\left(\phi_h(t) + (\upsilon_h + \varpi)\right) exp\left(\int_0^t \phi_h(\tau)d\tau + (\upsilon_h + \varpi)t\right) \\
&exp\left(\int_0^t \phi_h(\tau)d\tau + (\upsilon_h + \varpi)t\right) \times \left(\frac{dS_h(t)}{dt} + (\phi_h + (\upsilon_h + \varpi)) S_h(t)\right) \geq 0.
\end{aligned} \tag{3.9}$$

This means that

$$\frac{d}{dt}\left[S_h(t) exp\left(\int_0^t (\phi_h(\tau)d\tau + (\upsilon_h + \varpi)t\right)\right] \geq 0. \tag{3.10}$$

When the inequality above is integrated from zero 0 to t_1, it yields

$$\int_0^{t_1} \left[S_h(t) exp\left(\int_0^t \phi_h(\tau)d\tau + (\upsilon_h + \varpi)t\right)\right] \geq 0, \tag{3.11}$$

or alternatively,

$$S_h(t_1) exp\left(\int_0^{t_1} \phi_h(\tau)d\tau + (\upsilon_h + \varpi)t_1\right) - S_h(0) \geq 0, \tag{3.12}$$

becomes

$$S_h(t_1) \geq exp\left(-(\upsilon_h + \varpi)t_1 - \int_0^{t_1} \phi_h(\tau)d\tau\right) S_h(0) > 0, \tag{3.13}$$

which might counter the assertion that $S_h(t_1) = 0$. The remaining scenarios $E_h(t_1), V_h(t_1) = 0, I_h(t_1) = 0, R_h(t_1) = 0, S_r(t_1) = 0, E_r(t_1) = 0$, and $I_r(t_1) = 0$ result in the same contradiction. Consequently, $S_h(t) > 0$,$E_h(t) > 0$, $V_h(t) > 0, I_h(t) > 0, R_h(t) > 0, S_r(t) > 0, E_r(t) > 0$, and $I_r(t) > 0$ for all $t > 0$. □

Theorem 3.3. *Every non-negative solution to the model* (2.1) *is drawn to the positively invariant region* $\mathcal{D}$.

Proof. Let

$$\mathcal{D} = \mathcal{D}_h \times \mathcal{D}_r,$$

$$\mathcal{D}_h = \{(S_h, E_h, V_h, I_h, R_h) \in R_+^5 : M_h \leq \frac{\Phi_h}{\upsilon_h}\},$$

and

$$\mathcal{D}_r = \{(S_r, E_r, I_r) \in R_+^3 : M_r \leq \frac{\Phi_r}{\upsilon_r}\}.$$

When $0 \leq M_h(0) \leq \frac{\Phi_h}{\upsilon_h}$, and $0 \leq M_r(0) \leq \frac{\Phi_r}{\upsilon_r}$, we must demonstrate that the entire HUM population at time t, $M_h(t)$, and the entire rodents population $M_r(t)$ meets the boundedness property $0 \leq M_h(0) \leq \frac{\Phi_h}{\upsilon_h}$, and $0 \leq M_r(0) \leq \frac{\Phi_r}{\upsilon_r}$, respectively. We note that under the ideal scenario, in which there are no active disease misuse cases, this bound represents the unique equilibrium of the dynamics of the entire population. The conservation law [31] can be obtained by inserting the model's equation (2.1). Since our major goal was to demonstrate that any solution in $\mathcal{D}$ stays in $\mathcal{D}$, the rate of change within the entire HUM population is indicated by

$$\frac{dM_h}{dt} = \Phi_h - \upsilon_h M_h - \delta_h I_h \leq \Phi_h - \upsilon_h M_h. \tag{3.14}$$

Equation (3.14) may be solved using the Groomwall inequality to obtain

$$M_h(t) \leq \frac{\Phi_h}{\upsilon_h} + \left[M_h(0) - \frac{\Phi_h}{\upsilon_h}\right] e^{-\upsilon t}, \forall t \geq 0. \tag{3.15}$$

This suggests that $0 \leq M_h(t) \leq \frac{\Phi_h}{\upsilon_h}$ whenever $0 \leq M_h(0) \leq \frac{\Phi_h}{\upsilon_h}$ $\forall t \geq 0$, or, to put it another way, from (3.15), as $t \to 0$, $M_h(t) \to M_h(0) \Rightarrow M_h(t) \leq \frac{\Phi_h}{\upsilon_h}$, and $t \to \infty$ $M_h(t) \to \frac{\Phi_h}{\upsilon_h}$.

For the rodent population, since our major goal was to demonstrate that any solution in $\mathcal{D}$ stays in $\mathcal{D}$, the pace at which the entire rodent population is changing is provided by

$$\frac{dM_r}{dt} = \Phi_r - \upsilon_r M_r. \tag{3.16}$$

Equation (3.16) may be solved using the Groomwall inequality to obtain

$$M_r(t) \leq \frac{\Phi_r}{\upsilon_r} + \left[M_r(0) - \frac{\Phi_r}{\upsilon_r}\right] e^{-\upsilon t}, \forall t \geq 0. \tag{3.17}$$

This suggests that $0 \leq M_r(t) \leq \frac{\Phi_r}{\upsilon_r}$ whenever $0 \leq M_r(0) \leq \frac{\Phi_r}{\upsilon_r}$ $\forall t \geq 0$, or, to put it another way from (3.17), as $t \to 0$, $M_r(t) \to M_r(0) \Rightarrow M_r(t) \leq \frac{\Phi_r}{\upsilon_r}$ and $t \to \infty$ $M_r(t) \to \frac{\Phi_r}{\upsilon_r}$.

Thus, for any positive initial conditions, $\mathcal{D}$ is positively invariant and a global attractor of all positive solutions of the model (2.1). □

3.3. Existence of arbitrary equilibrium

Let $\mathcal{D}^* = (S_H^*, E_h^*, V_h^*, I_h^*, R_h^*, S_r^*, E_r^*, I_r^*)$ be an arbitrary equilibrium. We solved the equilibrium point by setting the right-hand side of model (2.1) to zero, and solving simultaneously at the arbitrary equilibrium using Maple software. We have

$$\begin{aligned}
S_h^* =& \frac{\sigma_2\sigma_3\Phi_h}{\left(\left(\phi_h^* + \sigma_1\right)\sigma_3 - \vartheta\,\varpi\right)\sigma_2 - \vartheta\,\mu\,\phi_h^*},\\
E_h^* =& \frac{\phi_h^*\sigma_3\Phi_h}{\left(\left(\phi_h^* + \sigma_1\right)\sigma_3 - \vartheta\,\varpi\right)\sigma_2 - \vartheta\,\mu\,\phi_h^*},\\
V_h^* =& \frac{\Phi_h\left(\varpi\,\sigma_2 + \mu\,\phi_h^*\right)}{\left(\left(\phi_h^* + \sigma_1\right)\sigma_3 - \vartheta\,\varpi\right)\sigma_2 - \vartheta\,\mu\,\phi_h^*},\\
I_h^* =& \frac{p_h\,(1-\psi)\,\phi_h^*\sigma_3\Phi_h}{\sigma_4\left(\left(\left(\phi_h^* + \sigma_1\right)\sigma_3 - \vartheta\,\varpi\right)\sigma_2 - \vartheta\,\mu\,\phi_h^*\right)},\\
R_h^* =& \frac{\tau p_h\,(1-\psi)\,\phi_h^*\sigma_3\Phi_h}{\upsilon_h\sigma_4\left(\left(\left(\phi_h^* + \sigma_1\right)\sigma_3 - \vartheta\,\varpi\right)\sigma_2 - \vartheta\,\mu\,\phi_h^*\right)}\\
&+\frac{\gamma p_h\,(1-\psi)\,\phi_h^*\sigma_3\Phi_h}{\upsilon_h\left(\left(\left(\phi_h^* + \sigma_1\right)\sigma_3 - \vartheta\,\varpi\right)\sigma_2 - \vartheta\,\mu\,\phi_h^*\right)}\\
&+\frac{p_h\psi p_h\,(1-\psi)\,\phi_h^*\sigma_3\Phi_h}{\upsilon_h\left(\left(\left(\phi_h^* + \sigma_1\right)\sigma_3 - \vartheta\,\varpi\right)\sigma_2 - \vartheta\,\mu\,\phi_h^*\right)}\\
S_r^* =& \frac{\Phi_r}{(\phi_r^* + \upsilon_r)}, E_r^* = \frac{\Phi_r\phi_r^*}{\sigma_5(\phi_r^* + \upsilon_r)}, I_r^* = \frac{p_r\Phi_r\phi_r^*}{\upsilon_r\sigma_5(\phi_r^* + \upsilon_r)}.
\end{aligned} \tag{3.18}$$

Now, ϕ_r at an arbitrary equilibrium is given as

$$\phi_r^* = \frac{\varrho_r I_r^*}{M_r^*} = \frac{\varrho_r I_r^*}{S_r^* + E_r^* + I_r^*}. \tag{3.19}$$

Substituting the concerned variable in (3.18) into Eq (3.19), we have

$$\phi_r^*\left(\Phi_r(\upsilon_r + p_r)\phi_r^* + \Phi_r(\upsilon_r\sigma_5 - \varrho_r p_r)\right) = 0, \tag{3.20}$$

and either

$$\phi_r^* = 0, \tag{3.21}$$

or

$$\Phi_r(\upsilon_r + p_r)\phi_r^* + \Phi_r(\upsilon_r\sigma_5 - \varrho_r p_r) = 0. \tag{3.22}$$

Solving, Eq (3.22), gives

$$\phi_r^* = \frac{\upsilon_r\sigma_5\left(\frac{\varrho_r p_r}{\upsilon_r\sigma_5} - 1\right)}{\upsilon_r + p_r}. \tag{3.23}$$

Now, ϕ_h at an arbitrary equilibrium is given as

$$\phi_h^* = \frac{(1-\chi)\varrho_h(I_h^* + \alpha I_r^*)}{M_h^*} = \frac{(1-\chi)\varrho_h(I_h^* + \alpha I_r^*)}{S_h^* + E_h^* + V_h^* + I_h^* + R_h^*}, \tag{3.24}$$

and by substituting the concerned variable in (3.18) into Eq (3.24), we have

$$\phi_h^*\left(A_1\phi_h^* + A_2\right) = 0, \tag{3.25}$$

where

$$\begin{aligned} A_1 =& \upsilon_h\upsilon_r\sigma_2\sigma_3\sigma_4\sigma_5\Phi_h + \upsilon_h\upsilon_r\sigma_3\sigma_4\sigma_5\Phi_h\phi_r^* + \upsilon_h\upsilon_r\sigma_3\sigma_4\sigma_5\Phi_h\upsilon_r + \upsilon_h\upsilon_r\mu\sigma_4\sigma_5\Phi_h\phi_r^* \\ &+ \upsilon_h\upsilon_r\mu\sigma_4\sigma_5\Phi_h\upsilon_r + \upsilon_h p_h(1-\psi)\upsilon_r\sigma_3\sigma_5\Phi_h\phi_r^* + \upsilon_h p_h(1-\psi)\upsilon_r\sigma_3\sigma_5\Phi_h\upsilon_r \\ &+ \tau p_h(1-\psi)\upsilon_r\sigma_3\sigma_5\Phi_h\phi_r^* + \tau p_h(1-\psi)\upsilon_r\sigma_3\sigma_5\Phi_h\upsilon_r + \gamma p_h(1-\psi)\upsilon_r\sigma_3\sigma_5\Phi_h\phi_r^* \\ &+ \gamma p_h(1-\psi)\upsilon_r\sigma_3\sigma_5\Phi_h\upsilon_r + p_h\psi p_h(1-\psi)\upsilon_r\sigma_3\sigma_5\Phi_h\phi_r^* + p_h\psi p_h(1-\psi)\upsilon_r\sigma_3\sigma_5\Phi_h\upsilon_r \\ &- (1-\chi)\varrho_h p_h(1-\psi)\sigma_3\sigma_5\upsilon_h\upsilon_r\Phi_h\phi_r^* - (1-\chi)\varrho_h\alpha\sigma_2\sigma_3\sigma_4 p_r\upsilon_h\Phi_h\phi_r^* \\ A_2 =& \sigma_4\sigma_2\left(\sigma_1\sigma_3 - \vartheta\varpi\right) - p_h\upsilon_h\sigma_3\varrho_h\left(1-\psi\right)\left(1-\chi\right) \\ =& \sigma_4\sigma_2\left(\sigma_1\sigma_3 - \vartheta\varpi\right)\left(1 - \frac{p_h\upsilon_h\sigma_3\varrho_h\left(1-\psi\right)\left(1-\chi\right)}{\sigma_4\sigma_2\left(\sigma_1\sigma_3 - \vartheta\varpi\right)}\right), \end{aligned} \tag{3.26}$$

and either

$$\phi_h^* = 0, \tag{3.27}$$

or

$$A_1\phi_h^* + A_2 = 0. \tag{3.28}$$

3.4. Disease-free equilibrium

In (3.29), the disease free equilibrium (DFE) of model (2.1) is shown.

$$\begin{aligned} \mathcal{D}^0 &= (S_h^0, E_h^0, V_h^0, I_h^0, R_h^0, S_r^0 E_r^0, I_r^0) \\ &= \left(\frac{\Phi_h(\upsilon_h+\gamma)}{(\upsilon_h+\gamma)(\upsilon_h+\varpi) - \vartheta\varpi}, 0, \frac{\varpi\Phi_h(\upsilon_h+\gamma)}{(\upsilon_h+\gamma)(\upsilon_h+\varpi) - \vartheta\varpi}, 0, \frac{\gamma\varpi\Phi_h(\upsilon_h+\gamma)}{\upsilon_h\left((\upsilon_h+\gamma)(\upsilon_h+\varpi) - \vartheta\varpi\right)}, \frac{\Phi_r}{\upsilon_r}, 0, 0\right). \end{aligned} \tag{3.29}$$

3.5. Local stability and basic reproduction number

Model (2.1) was subjected to the next-generation operator method [32–34] to establish local stability of $\mathcal{D}^0$ using the notation as in [33, 35]: the matrices F and V for the new infection terms and the remaining transfer terms to obtain the reproduction number, which is given by

$$F = \begin{bmatrix} 0 & \frac{\varrho_h(1-\chi)S_h^0}{M_h^0} & 0 & \frac{\varrho_h\alpha(1-\chi)S_h^0}{M_h^0} \\ 0 & 0 & 0 & 0 \\ 0 & 0 & 0 & \frac{\varrho_r S_r^0}{M_r^0} \\ 0 & 0 & 0 & 0 \end{bmatrix}. \tag{3.30}$$

Substituting the values of S_h^0, M_h^0, S_r^0 and M_r^0 into matrix (3.30), leads to the following matrix:

$$F = \begin{bmatrix} 0 & \frac{\varrho_h(1-\chi)\sigma_3\upsilon_h}{\sigma_1\sigma_3-\vartheta\varpi} & 0 & \frac{\varrho_h\alpha(1-\chi)\sigma_3\upsilon_h}{\sigma_1\sigma_3-\vartheta\varpi} \\ 0 & 0 & 0 & 0 \\ 0 & 0 & 0 & \varrho_r \\ 0 & 0 & 0 & 0 \end{bmatrix}, \tag{3.31}$$

and

$$V = \begin{bmatrix} \sigma_2 & 0 & 0 & 0 \\ -p_h(1-\psi) & \sigma_4 & 0 & 0 \\ 0 & 0 & \sigma_5 & 0 \\ 0 & 0 & -p_r & \upsilon_r \end{bmatrix}. \tag{3.32}$$

Then V^{-1} is given by

$$V^{-1} = \begin{bmatrix} {\sigma_2}^{-1} & 0 & 0 & 0 \\ -\frac{p_h(-1+\psi)}{\sigma_2\sigma_4} & {\sigma_4}^{-1} & 0 & 0 \\ 0 & 0 & {\sigma_5}^{-1} & 0 \\ 0 & 0 & \frac{p_r}{\sigma_5\upsilon_r} & {\upsilon_r}^{-1} \end{bmatrix}. \tag{3.33}$$

Furthermore, FV^{-1} can be given as

$$FV^{-1} = \begin{bmatrix} -\frac{\varrho_h(1-\chi)\sigma_3\upsilon_h p_h(-1+\psi)}{(\sigma_1\sigma_3-\vartheta\varpi)\sigma_2\sigma_4} & \frac{\varrho_h(1-\chi)\sigma_3\upsilon_h}{(\sigma_1\sigma_3-\vartheta\varpi)\sigma_4} & \frac{\varrho_h\alpha(1-\chi)\sigma_3\upsilon_h p_r}{(\sigma_1\sigma_3-\vartheta\varpi)\sigma_5\upsilon_r} & \frac{\varrho_h\alpha(1-\chi)\sigma_3\upsilon_h}{(\sigma_1\sigma_3-\vartheta\varpi)\upsilon_r} \\ 0 & 0 & 0 & 0 \\ 0 & 0 & \frac{\varrho_r p_r}{\sigma_5\upsilon_r} & \frac{\varrho_r}{\upsilon_r} \\ 0 & 0 & 0 & 0 \end{bmatrix}. \tag{3.34}$$

Then, the eigenvalues are given below:

$$\begin{bmatrix} 0 \\ 0 \\ \frac{\varrho_r p_r}{\sigma_5\upsilon_r} \\ \frac{p_h\upsilon_h\sigma_3\varrho_h(1-\psi-\chi+\chi\psi)}{\sigma_4\sigma_2(\sigma_1\sigma_3-\vartheta\varpi)} \end{bmatrix}. \tag{3.35}$$

Taking the maximum of the eigenvalues of (3.34) gives

$$\begin{aligned} \rho(FV^{-1}) = \mathcal{R}_c &= \left\{ \frac{p_h\upsilon_h\sigma_3\varrho_h(1-\psi-\chi+\chi\psi)}{\sigma_4\sigma_2(\sigma_1\sigma_3-\vartheta\varpi)}, \frac{\varrho_r p_r}{\sigma_5\upsilon_r} \right\} \\ &= \left\{ \mathcal{R}_c^h, \mathcal{R}_0^r \right\}, \end{aligned} \tag{3.36}$$

where

$$\sigma_1 = \upsilon_h + \varpi, \sigma_2 = p_h + \upsilon_h + \mu, \sigma_3 = \vartheta + \upsilon_h + \gamma, \sigma_4 = \upsilon_h + \delta_h + \tau, \sigma_5 = p_r + \upsilon_r,$$

$$\begin{aligned}\mathcal{R}_c^h =& \frac{p_h\upsilon_h\sigma_3\varrho_h\left(1-\psi-\chi+\chi\,\psi\right)}{\sigma_4\sigma_2\left(\sigma_1\sigma_3-\vartheta\,\varpi\right)} = \frac{p_h\upsilon_h\sigma_3\varrho_h\left(1-\psi\right)\left(1-\chi\right)}{\sigma_4\sigma_2\left(\sigma_1\sigma_3-\vartheta\,\varpi\right)},\\ \mathcal{R}_0^r =& \frac{\varrho_r p_r}{\sigma_5\upsilon_r}.\end{aligned} \tag{3.37}$$

Epidemiological interpretation of effective reproduction number ($\mathcal{R}_c$): The effective reproduction number, or $\mathcal{R}_c$, is the number of new infections brought on by infected people in a society composed of susceptible individuals. In other words, it is the quantity of infections that an infected individual produces when there are interpersonal controls present. Therefore, we assert the following outcome using Theorem 2 in [25, 33].

3.6. Local stability of disease-free equilibrium

In this subsection, the local stability of disease-free equilibrium will be discussed using the Jacobian matrix method.

Theorem 3.4. *If the effective reproduction number is less than or equal to one (1) ($\mathcal{R}_c \leq 1$), then the DFE (disease-free equilibrium) of Model* (2.1) *is LAS (locally asymptotically stable).*

Proof. $J(\mathcal{D}^0)$ is the Jacobian matrix of model (2.1) evaluated at disease-free equilibrium.

$$J(\mathcal{D}^0) = \begin{bmatrix} -\sigma_1 & 0 & \upsilon & -\pi_1 & 0 & 0 & 0 & -\pi_1\alpha \\ 0 & -\sigma_2 & 0 & \pi_1 & 0 & 0 & 0 & \pi_1\alpha \\ \varpi & \mu & -\sigma_3 & 0 & 0 & 0 & 0 & 0 \\ 0 & p_h\left(1-\psi\right) & 0 & -\sigma_4 & 0 & 0 & 0 & 0 \\ 0 & p_h\psi & \gamma & \tau & -\upsilon_h & 0 & 0 & 0 \\ 0 & 0 & 0 & 0 & 0 & -\upsilon_r & 0 & \varrho_r \\ 0 & 0 & 0 & 0 & 0 & 0 & -\sigma_5 & \varrho_r \\ 0 & 0 & 0 & 0 & 0 & 0 & p_r & -\upsilon_r \end{bmatrix}, \tag{3.38}$$

where

$$\pi_1 = \frac{\varrho_h\left(1-\chi\right)\sigma_3\upsilon_h}{\sigma_1\sigma_3-\vartheta\,\varpi}. \tag{3.39}$$

We found an upper triangular matrix of matrix (3.38) using Maple 13 software, which is given below:

$$\begin{bmatrix} -\sigma_1 & 0 & \upsilon & -\pi_1 & 0 & 0 & 0 & -\pi_1\alpha \\ 0 & -\sigma_2 & 0 & \pi_1 & 0 & 0 & 0 & \pi_1\alpha \\ 0 & 0 & \frac{-\sigma_3\sigma_1+\varpi\,\upsilon}{\sigma_1} & \frac{\pi_1(-\varpi\,\sigma_2+\mu\,\sigma_1)}{\sigma_1\sigma_2} & 0 & 0 & 0 & \frac{\pi_1\alpha\,(-\varpi\,\sigma_2+\mu\,\sigma_1)}{\sigma_1\sigma_2} \\ 0 & 0 & 0 & \frac{-\sigma_4\sigma_2-p_h(-1+\psi)\pi_1}{\sigma_2} & 0 & 0 & 0 & -\frac{p_h(-1+\psi)\pi_1\alpha}{\sigma_2} \\ 0 & 0 & 0 & 0 & -\upsilon_h & 0 & 0 & -\Gamma \\ 0 & 0 & 0 & 0 & 0 & -\upsilon_r & 0 & \varrho_r \\ 0 & 0 & 0 & 0 & 0 & 0 & -\sigma_5 & \varrho_r \\ 0 & 0 & 0 & 0 & 0 & 0 & 0 & \frac{-\upsilon_r\sigma_5+p_r\varrho_r}{\sigma_5} \end{bmatrix}, \tag{3.40}$$

where

$$\Gamma = \frac{\pi_1 \left((-\psi\,\sigma_4 + \tau\,(-1+\psi))\,(-\sigma_3\sigma_1 + \varpi\,\upsilon)\,p_h + \gamma\,\sigma_4\,(-\varpi\,\sigma_2 + \mu\,\sigma_1)\right)\alpha}{(-\sigma_3\sigma_1 + \varpi\,\upsilon)\,(p_h\,(-1+\psi)\,\pi_1 + \sigma_4\sigma_2)}. \tag{3.41}$$

Now, the eigenvalues are as given below:

$$\begin{bmatrix} \lambda_1 = -\upsilon_r \\ \lambda_2 = -\upsilon_h \\ \lambda_3 = -\sigma_5 \\ \lambda_4 = -\sigma_1 \\ \lambda_5 = -\frac{\sigma_3\sigma_1 - \varpi\,\upsilon}{\sigma_1} \\ \lambda_6 = -\sigma_2 \\ \lambda_7 = \frac{-\upsilon_r\sigma_5 + p_r\varrho_r}{\sigma_5} \\ \lambda_8 = -\frac{\sigma_4\sigma_2 - p_h\pi_1 + p_h\pi_1\psi}{\sigma_2}, \end{bmatrix}. \tag{3.42}$$

We observed from the matrix (3.42) above that all the eigenvalues are negative except λ_7 and λ_8. Now, substituting the value of π_1 into λ_8, we have

$$\lambda_8 = \frac{-\sigma_4\sigma_2 + \frac{p_h\pi_1(1-\psi)\varrho_h(1-\chi)\sigma_3\upsilon_h}{(\sigma_1\sigma_3 - \vartheta\varpi)}}{\sigma_2}. \tag{3.43}$$

Re-simplifying Eq (3.43), we have

$$\begin{aligned} \lambda_8 =& \frac{-\sigma_4\sigma_2\left(1 - \frac{p_h\pi_1(1-\psi)\varrho_h(1-\chi)\sigma_3\upsilon_h}{\sigma_4\sigma_2(\sigma_1\sigma_3 - \vartheta\varpi)}\right)}{\sigma_2} \\ =& -\sigma_4\left(1 - \frac{p_h\pi_1(1-\psi)\varrho_h(1-\chi)\sigma_3\upsilon_h}{\sigma_4\sigma_2(\sigma_1\sigma_3 - \vartheta\varpi)}\right) \\ =& -\sigma_4\left(1 - \mathcal{R}_c^h\right). \end{aligned} \tag{3.44}$$

It is obvious from Eq (3.44) that $\lambda_8 < 0$ if and only if $\mathcal{R}_c^h < 1$. Now, for λ_7,

$$\begin{aligned} \lambda_7 =& \frac{-\upsilon_r\sigma_5 + p_r\varrho_r}{\sigma_5} \\ =& \frac{-\upsilon_r\sigma_5\left(1 - \frac{p_r\varrho_r}{\upsilon_r\sigma_5}\right)}{\sigma_5} \\ =& -\upsilon_r\left(1 - \mathcal{R}_0^r\right), \end{aligned} \tag{3.45}$$

it is obvious from Eq (3.45) that, $\lambda_7 < 0$ if and only if $\mathcal{R}_0^r < 1$. Therefore, we conclude that the disease-free equilibrium point is locally asymptotically stable if $\mathcal{R} < 1$, since by definition $\mathcal{R}_c = \left(\mathcal{R}_c^h, \mathcal{R}_0^r\right)$. □

3.7. Backward bifurcation analysis

This section will examine the coexistence of endemic equilibrium and disease-free equilibrium when $\mathcal{R}_c^h = 1$. Therefore, we claim the following result:

Theorem 3.5. *If bifurcation parameters a and b are positive, the model* (2.1) *exhibits backward bifurcation at* $\mathcal{R}_c^h = 1$.

Proof. Considering when $\mathcal{R}_c^h = 1$ by solving $\vartheta_h = \vartheta_h^*$, we obtain

$$\vartheta_h^* = \frac{\sigma_4\sigma_2(\sigma_1\sigma_3 - \vartheta\varpi)}{p_h\upsilon_h\sigma_3(1-\psi)(1-\chi)}. \tag{3.46}$$

Rewriting Eq (2.1) while taking into account $S_h = y_1, E_h = y_2, V_h = y_3, I_h = y_4, R_h = y_5, S_r = y_6, E_r = y_7$, and $I_r = y_8$, results in

$$\begin{aligned}
h_1 &= \dot{y}_1 = \Phi_h + \vartheta y_3 - \frac{(1-\chi)\varrho_h(y_4 + \alpha y_8)y_1}{y_1 + y_2 + \cdots + y_5} - k_1 y_1,\\
h_2 &= \dot{y}_2 = \frac{(1-\chi)\varrho_h(y_4 + \alpha y_8)y_1}{y_1 + y_2 + \cdots + y_5} - k_2 y_2,\\
h_3 &= \dot{y}_3 = \varpi y_1 + \mu y_2 - k_3 y_3,\\
h_4 &= \dot{y}_4 = p_h(1-\psi)y_2 - k_4 y_4,\\
h_5 &= \dot{y}_5 = \tau y_4 + \gamma y_3 + p_h\psi y_2 - \upsilon_h y_5,\\
h_6 &= \dot{y}_6 = \Phi_r - \frac{\varrho_r y_8 y_6}{y_6 + y_7 + y_8} - \upsilon y_6,\\
h_7 &= \dot{y}_7 = \frac{\varrho_r y_8 y_6}{y_6 + y_7 + y_8} - k_5 y_7,\\
h_8 &= \dot{y}_8 = p_r y_7 - \upsilon y_8.
\end{aligned} \tag{3.47}$$

With $\varrho_h = \varrho_h^*$, the Jacobian of the modified model at the DFE is provided by

$$\mathbf{J}_{\beta_C^*} = \begin{bmatrix}
-\sigma_1 & 0 & \vartheta & -\pi & 0 & 0 & 0 & -\pi\alpha\\
0 & -\sigma_2 & 0 & \pi & 0 & 0 & 0 & \pi\alpha\\
\varpi & \mu & -\sigma_3 & 0 & 0 & 0 & 0 & 0\\
0 & p_h(1-\psi) & 0 & -\sigma_4 & 0 & 0 & 0 & 0\\
0 & p_h\psi & \gamma & \tau & -\upsilon_h & 0 & 0 & 0\\
0 & 0 & 0 & 0 & 0 & -\upsilon_r & 0 & -\varrho_r\\
0 & 0 & 0 & 0 & 0 & 0 & -\sigma_5 & \varrho_r\\
0 & 0 & 0 & 0 & 0 & 0 & p_r & -\upsilon_r
\end{bmatrix}, \tag{3.48}$$

where

$$\pi = \frac{\varrho_h(1-\chi)\sigma_3\upsilon_h}{\sigma_1\sigma_3 - \vartheta\varpi}. \tag{3.49}$$

The following are $\mathbf{J}_{\varrho_h^*}$'s right eigenvectors:

$$\begin{aligned}
\omega_6 &= \omega_7 = \omega_8 == 0,\\
\omega_3 &= \frac{(\varpi+\mu)\omega_2}{\sigma_3},\\
\omega_1 &= \omega_2 > 0,\\
\omega_4 &= \frac{p_h(1-\psi)\omega_2}{\sigma_4}.\\
\omega_5 &= \frac{(\sigma_4\sigma 3 p_h\psi + \gamma\sigma_4(\varpi+\mu) + \sigma_3 p_h(1-\psi))\,\omega_2}{\sigma_3\sigma_4}.
\end{aligned} \tag{3.50}$$

The following are $\mathbf{J}_{\varrho_h^*}$'s left eigenvectors:

$$\begin{aligned}
v_1 &= \frac{\varpi v_2}{\sigma_1}, v_2 = v_3 > 0, v_4 = -\frac{\pi\varpi v_2}{\sigma_1\sigma_4},\\
v_5 &= v_6 = 0, v_7 = \frac{p_r v_8}{\sigma_5}, v_8 = v_8 > 0.
\end{aligned} \tag{3.51}$$

The associated non-zero partial derivatives of the right-hand sides of the transformed system (3.47) must be calculated using center manifold theory as in [36, 37]. These must be evaluated at the disease-free equilibrium with $\varrho_h = \varrho_h^*$, and the corresponding bifurcation coefficients, a and b, are provided by

$$\begin{aligned}
a &= \sum_{k,i,j=1}^{8} v_k\omega_i\omega_j\frac{\partial^2 h_k}{\partial y_i\partial y_j}\\
b &= \sum_{k,i,=1}^{8} v_k\omega_i\frac{\partial^2 h_k}{\partial y_i\partial \varrho_h^*}.
\end{aligned} \tag{3.52}$$

Computation of a.

The corresponding non-zero partial derivatives for the modified system (3.47) are provided as

$$\begin{aligned}
&\frac{\partial^2 h_1}{\partial y_2\partial y_8} = \frac{\partial^2 h_1}{\partial y_8\partial y_2} = \frac{\partial^2 h_1}{\partial y_4\partial y_8} = \frac{\partial^2 h_1}{\partial y_8\partial y_4} = \frac{\partial^2 h_1}{\partial y_5\partial y_8} = \frac{\partial^2 h_1}{\partial y_8\partial y_5} = \frac{\partial^2 h_1}{\partial y_3\partial y_8} = \frac{\partial^2 h_1}{\partial y_8\partial y_3} = \frac{(1-\chi)\varrho_h\alpha}{S_h^0},\\
&\frac{\partial^2 h_1}{\partial y_2\partial y_4} = \frac{\partial^2 h_1}{\partial y_4\partial y_8} = \frac{\partial^2 h_1}{\partial y_4\partial y_3} = \frac{\partial^2 h_1}{\partial y_3\partial y_4} = \frac{\partial^2 h_1}{\partial y_5\partial y_4} = \frac{\partial^2 h_1}{\partial y_4\partial y_5} = \frac{(1-\chi)\varrho_h}{S_h^0},\\
&\frac{\partial^2 h_1}{\partial y_4\partial y_4} = -\frac{\partial^2 h_2}{\partial y_4\partial y_4} = \frac{2(1-\chi)\varrho_h}{S_h^0},\\
&\frac{\partial^2 h_2}{\partial y_2\partial y_8} = \frac{\partial^2 h_2}{\partial y_8\partial y_2} = \frac{\partial^2 h_2}{\partial y_4\partial y_8} = \frac{\partial^2 h_2}{\partial y_8\partial y_4} = \frac{\partial^2 h_2}{\partial y_5\partial y_8} = \frac{\partial^2 h_2}{\partial y_8\partial y_5} = \frac{\partial^2 h_2}{\partial y_3\partial y_8} = \frac{\partial^2 h_2}{\partial y_8\partial y_3} = -\frac{(1-\chi)\varrho_h\alpha}{S_h^0},\\
&\frac{\partial^2 h_2}{\partial y_2\partial y_4} = \frac{\partial^2 h_2}{\partial y_4\partial y_8} = \frac{\partial^2 h_2}{\partial y_4\partial y_3} = \frac{\partial^2 h_2}{\partial y_3\partial y_4} = \frac{\partial^2 h_2}{\partial y_5\partial y_4} = \frac{\partial^2 h_2}{\partial y_4\partial y_5} = -\frac{(1-\chi)\varrho_h}{S_h^0},\\
&\frac{\partial^2 h_6}{\partial y_6\partial y_6} = \frac{\partial^2 h_6}{\partial y_8\partial y_8} = \frac{2\varrho_r\upsilon_r}{\Phi_r} = -\frac{\partial^2 h_7}{\partial y_8\partial y_8} = -\frac{\partial^2 h_7}{\partial y_6\partial y_6},\\
&\frac{\partial^2 h_6}{\partial y_7\partial y_8} = \frac{\partial^2 h_6}{\partial y_8\partial y_7} = \frac{\varrho_r\upsilon_r}{\Phi_r} = -\frac{\partial^2 h_7}{\partial y_7\partial y_8} = -\frac{\partial^2 h_7}{\partial y_8\partial y_7}.
\end{aligned} \tag{3.53}$$

Following several algebraic operations, the aforementioned formulas indicate that

$$\begin{aligned} a &= v_1 \sum_{i,j=1}^{8} \omega_i \omega_j \frac{\partial^2 h_1}{\partial y_i \partial y_j} + v_2 \sum_{i,j=1}^{8} \omega_i \omega_j \frac{\partial^2 h_2}{\partial y_i \partial y_j} \\ &= v_1 \omega_2 \omega_4 \frac{\partial^2 h_1}{\partial y_2 \partial y_4} + v_2 \omega_4 \omega_2 \frac{\partial^2 h_1}{\partial y_4 \partial y_2} + v_2 \omega_4^2 \frac{\partial^2 h_1}{\partial y_4 \partial y_4} + v_1 \omega_3 \omega_4 \frac{\partial^2 h_1}{\partial y_3 \partial y_4} \\ &+ v_1 \omega_4 \omega_3 \frac{\partial^2 h_1}{\partial y_4 \partial y_3} + v_1 \omega_5 \omega_4 \frac{\partial^2 h_1}{\partial y_5 \partial y_4} + v_1 \omega_4 \omega_5 \frac{\partial^2 h_1}{\partial y_4 \partial y_5} + v_2 \omega_4^2 \frac{\partial^2 h_2}{\partial y_4 \partial y_4} \\ &+ v_2 \omega_4 \omega_2 \frac{\partial^2 h_2}{\partial y_4 \partial y_4} v_2 \omega_2 \omega_4 \frac{\partial^2 h_2}{\partial y_2 \partial y_4} + v_2 \omega_4 \omega_3 \frac{\partial^2 h_2}{\partial y_4 \partial y_3} + v_2 \omega_3 \omega_4 \frac{\partial^2 h_2}{\partial y_3 \partial y_4} \\ &+ v_2 \omega_4 \omega_5 \frac{\partial^2 h_2}{\partial y_4 \partial y_5} + v_2 \omega_5 \omega_4 \frac{\partial^2 h_2}{\partial y_5 \partial y_4}. \end{aligned} \tag{3.54}$$

Furthermore, substituting all the concern left and right eigen-vectors, and non-zero partial derivatives into Eq (3.54), we have

$$\begin{aligned} a &= \frac{4\varpi v_2^2 \omega_2 p_h (1-\psi)(1-\chi)\varrho_h}{\sigma_1 \sigma_4 S_h^0} + \frac{2\varpi v_2^2 \omega_2 p_h^2 (1-\psi)^2 (1-\chi)\varrho_h}{\sigma_1 \sigma_4^2 S_h^0} \\ &+ \frac{2\varpi v_2^2 p_h (1-\psi)(1-\chi)\varrho_h}{\sigma_1 \sigma_4 S_h^0} \times \frac{(\sigma_3 \sigma_4 \psi + \gamma(\varpi+\mu)\sigma_4 + \sigma_3 p_h (1-\psi) v_2)\,\omega_2}{\sigma_3 \sigma_4} \\ &- \frac{4 v_2^2 \omega_2 p_h (1-\psi)(1-\chi)\varrho_h \alpha}{\sigma_4 S_h^0} - \frac{2 v_2^3 \omega_2 p_h^2 (1-\psi)^2 (1-\chi)\varrho_h \alpha}{\sigma_4^2 S_h^0} \\ &- \frac{2 v_2^2 p_h (1-\psi)(1-\chi)\varrho_h \alpha}{\sigma_1 \sigma_4 S_h^0} \times \frac{(\sigma_3 \sigma_4 \psi + \gamma(\varpi+\mu)\sigma_4 + \sigma_3 p_h (1-\psi) v_2)\,\omega_2}{\sigma_3 \sigma_4}. \end{aligned} \tag{3.55}$$

Therefore, simplifying Eq (3.55), we obtained

$$\begin{aligned} a &= \frac{2\varpi v_2^2 \omega_2 p_h (1-\psi)(1-\chi)\varrho_h}{\sigma_1 \sigma_4 S_h^0} \left(2 + \frac{p_h (1-\psi) v_2}{\sigma_4} + \frac{(\sigma_3 \sigma_4 \psi + \gamma(\varpi+\mu)\sigma_4 + \sigma_3 p_h (1-\psi) v_2)\,\sigma_1}{\sigma_3 \sigma_4}\right) \\ &- \frac{2 v_2^2 \omega_2 p_h (1-\psi)(1-\chi)\varrho_h \alpha}{\sigma_4 S_h^0} \left(2 + \frac{p_h (1-\psi) v_2}{\sigma_4} + \frac{(\sigma_3 \sigma_4 \psi + \gamma(\varpi+\mu)\sigma_4 + \sigma_3 p_h (1-\psi) v_2)}{\sigma_3 \sigma_4}\right). \end{aligned} \tag{3.56}$$

Using the parameter b to calculate a bifurcation parameter, $\varrho_h = \varrho_h^*$, we have

$$\frac{\partial^2 h_1}{\partial y_4 \partial \varrho_h^*} = -(1-\chi), \frac{\partial^2 2_2}{\partial y_4 \partial \varrho_h^*} = (1-\chi). \tag{3.57}$$

It is evident from the aforementioned expressions that

$$\begin{aligned} b &= v_1 \sum_{i=1}^{8} \omega_i \frac{\partial^2 h_1}{\partial y_i \partial \varrho_h^*} + v_2 \sum_{i=1}^{8} \omega_i \frac{\partial^2 h_2}{\partial x_i \partial \varrho_h^*} \\ &= v_1 \omega_4 \frac{\partial^2 h_1}{\partial y_4 \partial \varrho_h^*} + v_2 \omega_4 \frac{\partial^2 h_2}{\partial y_4 \partial \varrho_h^*} \\ &= -\frac{\varpi v_2^2 p_h (1-\psi)(1-\chi)}{\sigma_1 \sigma_4} + \frac{v_2^2 p_h (1-\psi)(1-\chi)}{\sigma_4}. \end{aligned} \tag{3.58}$$

It is evident that for every biologically possible parameter value, $b > 0$ and $a < 0$, if $\varpi = 0$ (that is, when there is no imperfect vaccination). Thus, if and only if $a > 0$, we can say that backward bifurcation has occurred, but as we observed above, $a < 0$ if $\varpi = 0$. Therefore, the model does not possess backward bifurcation if $\varpi = 0$. □

Epidemiological implication: The implication of this result is that, with the presence of imperfect-vaccination in a population, Mpox can be transmitted behind the scenes, which will make the disease outbreak cyclic. But, if imperfect vaccination does not exist, it tends to help in reducing the transmission of disease in society.

3.8. Global stability of disease-free equilibrium

A dynamical system's global stability dictates whether or not it will continue to be stable even after more significant perturbations are made. Therefore, it is crucial to determine if the interventions included in the model can effectively control the Mpox infection for a significant number of infected people. Thus, we asserted the following theorem regarding the stability of model (2.1).

Theorem 3.6. *The disease-free equilibrium $\mathcal{D}^0$ of the model* (2.1) *is globally-asymptotically stable in region $\mathcal{D}$ if $\mathcal{R}_c < 1$ and unstable if $\mathcal{R}_c > 1$.*

Proof. The two axioms $[G_1]$ and $[G_2]$ for $\mathcal{R}_c < 1$ must be satisfied to demonstrate the global asymptotic stability of the disease-free equilibrium [38]. To facilitate analysis, model (2.1) is divided into two subsystems: $Z_1 = (S_h^0, V_h^0, R_h^0, S_r^0)$ and $Z_2 = (E_h^0, I_h^0, E_r^0, I_r^0)$. While the components of $Z_2 \in \mathbb{R}_+^4$ represent the infected classes, those of $Z_1 \in \mathbb{R}_+^4$ correspond to the uninfected subpopulation. It is possible to rewrite the model (2.1) as two connected differential equations, one guiding the dynamics of Z_1 and the other for Z_2, using this partition.

$$\begin{aligned} \frac{dZ_1}{dt} &= F(Z_1, Z_2), \\ \frac{dZ_2}{dt} &= G(Z_1, Z_2) : G(Z_1, 0) = 0. \end{aligned} \tag{3.59}$$

G_1: global stability of Z_1.

Now, the disease-free equilibrium can be expressed using the partitioned system as follows:

$$\mathcal{D}^0 = (Z_1, \mathbf{0}),$$

where all of the infected compartments have been reset to zero.

$$\frac{dZ_1}{dt} = F(Z_1, 0) = \begin{bmatrix} \Phi_h + \vartheta V_h^0 - (\upsilon_h + \varpi) S_h^0 \\ \varpi S_h^0 - (\upsilon_h + \gamma) V_h^0 \\ \gamma V_h^0 - \upsilon R_h^0 \\ \Phi_r - \upsilon_r S_r^0 \end{bmatrix}. \tag{3.60}$$

A linear ODE's solution in (3.60) produces

$$\begin{aligned}
\frac{\Phi_h + \vartheta V_h^0}{(\upsilon_h + \varpi)} - \frac{\Phi_h + \vartheta V_h^0}{(\upsilon_h + \varpi)} e^{-(\upsilon_h+\varpi)t} + S_h^0(0)e^{-(\upsilon_h+\varpi)t} &= S_h^0(t),\\
\frac{\varpi S_h^0}{(\upsilon_h + \gamma)} - \frac{\varpi S_h^0}{(\upsilon_h + \gamma)} e^{-(\upsilon_h+\gamma)t} + V_h^0(0)e^{-(\upsilon_h+\gamma)t} &= V_h^0(t),\\
\frac{\gamma V_h^0}{\upsilon_h} - \frac{\gamma V_h^0}{\upsilon_h} e^{-\upsilon_h t} + R_h^0(0)e^{-\upsilon_h t} &= R_h^0(t),\\
\frac{\Phi_r}{\upsilon_r} - \frac{\Phi_r}{\upsilon_r} e^{-\upsilon_r t} + S_r^0(0)e^{-\upsilon_r t} &= S_r^0(t).
\end{aligned} \tag{3.61}$$

It is evident from model (2.1) that as $t \to \infty$, the sum $S_h^0(t) + V_h^0(t) + R_h^0(t)$ approaches the total HUM population $M_h^0(t)$, and it is also evident from model (2.1) that as $t \to \infty$, the sum $S_r^0(t)$ approaches the total rodent population $M_r^0(t)$, regardless of the individual values of $S_h^0(t)$, $V_h^0(t)$, and $R_h^0(t)$. Consequently, the uninfected subsystem converges to $Z_1^* = (M_h^0/M_r^0, 0)$, which is globally asymptotically stable.

G_2**:**$\tilde{G}(Z_1, Z_2) = AZ_2 - G(Z_1, Z_2) \geq 0$

$$A = \begin{pmatrix} -(p_h + \upsilon_h + \mu) & \frac{\varrho_h(1-\xi)S_h}{M_h} & 0 & \frac{\alpha\varrho_h(1-\xi)S_h}{M_h} \\ p_h(1-\psi) & -(\upsilon_h + \tau + \delta_h) & 0 & 0 \\ 0 & o & -(p_r + \mu + \upsilon_r) & \frac{\varrho_r S_r}{M_r} \\ 0 & 0 & p_r & -\upsilon_r \end{pmatrix}. \tag{3.62}$$

The non-negativity of the off-diagonal elements of the matrix A makes it a Metzler matrix.

$$G(Z_1, Z_2) = \begin{pmatrix} \frac{\varrho_h(1-\chi)(I_h+\alpha I_r)}{M_h} S_h - (p_h + \upsilon_h + \mu)E_h \\ p_h(1-\psi)E_h - (\upsilon_h + \tau + \delta_h)I_h \\ \frac{\varrho_r I_r}{M_r} S_r - (p_r + \upsilon_r)E_r \\ p_r E_r - \upsilon_r I_r \end{pmatrix}. \tag{3.63}$$

Then,

$$\tilde{G}(Z_1, Z_2) = AZ_2 - G(Z_1, Z_2) = \begin{bmatrix} 0 \\ 0 \\ 0 \\ 0 \end{bmatrix}.$$

Therefore, $\tilde{G}(Z_1, Z_2) = 0$. □

Important epidemiological consequences result from Theorem (3.6), which states that regardless of the initial number of infected persons, Mpox may be eradicated by keeping the control reproduction number below unity ($\mathcal{R}_c < 1$). This suggests that even during major outbreaks, current measures, including treatment and early therapeutic education, can effectively prevent the spread of the disease.

3.9. Existence of endemic equilibrium point

In this subsection, the existence of an endemic equilibrium point will be assessed. First, we solved model (2.1) at the endemic equilibrium point using Maple 13 software. Now, let $\mathcal{D}^{**}$ be an endemic equilibrium point, which is given as

$$\mathcal{D}^{**} = (S_h^{**}, E_h^{**}, V_h^{**}, I_h^{**}, R_h^{**}, S_r^{**}, E_r^{**}, I_r^{**}). \tag{3.64}$$

Now, the endemic equilibrium points are given below:

$$\begin{aligned}
S_h^{**} =& \frac{\sigma_2\sigma_3\Phi_h}{\left(\left(\phi_h^{**}+\sigma_1\right)\sigma_3-\vartheta\varpi\right)\sigma_2-\vartheta\mu\phi_h^{**}},\\
E_h^{**} =& \frac{\phi_h^{**}\sigma_3\Phi_h}{\left(\left(\phi_h^{**}+\sigma_1\right)\sigma_3-\vartheta\varpi\right)\sigma_2-\vartheta\mu\phi_h^{**}},\\
V_h^{**} =& \frac{\Phi_h\left(\varpi\sigma_2+\mu\phi_h^{**}\right)}{\left(\left(\phi_h^{**}+\sigma_1\right)\sigma_3-\vartheta\varpi\right)\sigma_2-\vartheta\mu\phi_h^{**}},\\
I_h^{**} =& \frac{p_h(1-\psi)\phi_h^{**}\sigma_3\Phi_h}{\sigma_4\left(\left(\left(\phi_h^{**}+\sigma_1\right)\sigma_3-\vartheta\varpi\right)\sigma_2-\vartheta\mu\phi_h^{**}\right)},\\
R_h^{**} =& \frac{\tau p_h(1-\psi)\phi_h^{**}\sigma_3\Phi_h}{\upsilon_h\sigma_4\left(\left(\left(\phi_h^{**}+\sigma_1\right)\sigma_3-\vartheta\varpi\right)\sigma_2-\vartheta\mu\phi_h^{**}\right)}\\
&+\frac{\gamma p_h(1-\psi)\phi_h^{**}\sigma_3\Phi_h}{\upsilon_h\left(\left(\left(\phi_h^{**}+\sigma_1\right)\sigma_3-\vartheta\varpi\right)\sigma_2-\vartheta\mu\phi_h^{**}\right)}\\
&+\frac{p_h\psi p_h(1-\psi)\phi_h^{**}\sigma_3\Phi_h}{\upsilon_h\left(\left(\left(\phi_h^{**}+\sigma_1\right)\sigma_3-\vartheta\varpi\right)\sigma_2-\vartheta\mu\phi_h^{**}\right)}\\
S_r^{**} =& \frac{\Phi_r}{(\phi_r^{**}+\upsilon_r)}, E_r^{**} = \frac{\Phi_r\phi_r^{**}}{\sigma_5(\phi_r^{**}+\upsilon_r)}, I_r^{**} = \frac{p_r\Phi_r\phi_r^{**}}{\upsilon_r\sigma_5(\phi_r^{**}+\upsilon_r)}.
\end{aligned} \tag{3.65}$$

At the endemic equilibrium point, Eq (3.23) becomes

$$\phi_r^{**} = \frac{\upsilon_r\sigma_5\left(\frac{\varrho_r p_r}{\upsilon_r\sigma_5}-1\right)}{\sigma_5} = \upsilon_r\left(\mathcal{R}_0^r-1\right), \tag{3.66}$$

and at the endemic equilibrium point, Eq (3.27) becomes

$$A_1\phi_h^{**} + A_2 = 0, \tag{3.67}$$

where

$$\begin{aligned}
A_1 =&\upsilon_h\upsilon_r\sigma_2\sigma_3\sigma_4\sigma_5\Phi_h + \upsilon_h\upsilon_r\sigma_3\sigma_4\sigma_5\Phi_h\phi_r^{**} + \upsilon_h\upsilon_r\sigma_3\sigma_4\sigma_5\Phi_h\upsilon_r + \upsilon_h\upsilon_r\mu\sigma_4\sigma_5\Phi_h\phi_r^{**}\\
&+ \upsilon_h\upsilon_r\mu\sigma_4\sigma_5\Phi_h\upsilon_r + \upsilon_h p_h(1-\psi)\upsilon_r\sigma_3\sigma_5\Phi_h\phi_r^{**} + \upsilon_h p_h(1-\psi)\upsilon_r\sigma_3\sigma_5\Phi_h\upsilon_r\\
&+ \tau p_h(1-\psi)\upsilon_r\sigma_3\sigma_5\Phi_h\phi_r^{**} + \tau p_h(1-\psi)\upsilon_r\sigma_3\sigma_5\Phi_h\upsilon_r + \gamma p_h(1-\psi)\upsilon_r\sigma_3\sigma_5\Phi_h\phi_r^{**}\\
&+ \gamma p_h(1-\psi)\upsilon_r\sigma_3\sigma_5\Phi_h\upsilon_r + p_h\psi p_h(1-\psi)\upsilon_r\sigma_3\sigma_5\Phi_h\phi_r^{**} + p_h\psi p_h(1-\psi)\upsilon_r\sigma_3\sigma_5\Phi_h\upsilon_r\\
&- (1-\chi)\varrho_h p_h(1-\psi)\sigma_3\sigma_5\upsilon_h\upsilon_r\Phi_h\phi_r^{**} - (1-\chi)\varrho_h\alpha\sigma_2\sigma_3\sigma_4 p_r\upsilon_h\Phi_h\phi_r^{**},\\
A_2 =&\phi_r^{**}\sigma_4\sigma_2\left(\sigma_1\sigma_3 - \vartheta\varpi\right) - \phi_r^{**}p_h\upsilon_h\sigma_3\varrho_h\left(1-\psi\right)\left(1-\chi\right)\\
=&\,\phi_r^{**}\sigma_4\sigma_2\left(\sigma_1\sigma_3 - \vartheta\varpi\right)\left(1 - \frac{p_h\upsilon_h\sigma_3\varrho_h\left(1-\psi\right)\left(1-\chi\right)}{\sigma_4\sigma_2\left(\sigma_1\sigma_3 - \vartheta\varpi\right)}\right).
\end{aligned} \tag{3.68}$$

Therefore, (3.68), becomes

$$\begin{aligned}
A_1 =&\upsilon_h\upsilon_r\sigma_2\sigma_3\sigma_4\sigma_5\Phi_h + \upsilon_h\upsilon_r\sigma_3\sigma_4\sigma_5\Phi_h\phi_r^{**} + \upsilon_h\upsilon_r\sigma_3\sigma_4\sigma_5\Phi_h\upsilon_r + \upsilon_h\upsilon_r\mu\sigma_4\sigma_5\Phi_h\phi_r^{**}\\
&+ \upsilon_h\upsilon_r\mu\sigma_4\sigma_5\Phi_h\upsilon_r + \upsilon_h p_h(1-\psi)\upsilon_r\sigma_3\sigma_5\Phi_h\phi_r^{**} + \upsilon_h p_h(1-\psi)\upsilon_r\sigma_3\sigma_5\Phi_h\upsilon_r\\
&+ \tau p_h(1-\psi)\upsilon_r\sigma_3\sigma_5\Phi_h\phi_r^{**} + \tau p_h(1-\psi)\upsilon_r\sigma_3\sigma_5\Phi_h\upsilon_r + \gamma p_h(1-\psi)\upsilon_r\sigma_3\sigma_5\Phi_h\phi_r^{**}\\
&+ \gamma p_h(1-\psi)\upsilon_r\sigma_3\sigma_5\Phi_h\upsilon_r + p_h\psi p_h(1-\psi)\upsilon_r\sigma_3\sigma_5\Phi_h\phi_r^{**} + p_h\psi p_h(1-\psi)\upsilon_r\sigma_3\sigma_5\Phi_h\upsilon_r\\
&- (1-\chi)\varrho_h p_h(1-\psi)\sigma_3\sigma_5\upsilon_h\upsilon_r\Phi_h\phi_r^{**} - (1-\chi)\varrho_h\alpha\sigma_2\sigma_3\sigma_4 p_r\upsilon_h\Phi_h\phi_r^{**},\\
A_2 =&\phi_r^{**}\sigma_4\sigma_2\left(\sigma_1\sigma_3 - \vartheta\varpi\right)\left(1 - \mathcal{R}_c^h\right).
\end{aligned} \tag{3.69}$$

Now, substituting the value of (3.66) into (3.68), we have

$$\begin{aligned}
A_1 =&\upsilon_h\upsilon_r\sigma_2\sigma_3\sigma_4\sigma_5\Phi_h + \upsilon_h\upsilon_r\sigma_3\sigma_4\sigma_5\Phi_h\upsilon_r\left(\mathcal{R}_0^r - 1\right) + \upsilon_h\upsilon_r\sigma_3\sigma_4\sigma_5\Phi_h\upsilon_r + \upsilon_h\upsilon_r\mu\sigma_4\sigma_5\Phi_h\upsilon_r\left(\mathcal{R}_0^r - 1\right)\\
&+ \upsilon_h\upsilon_r\mu\sigma_4\sigma_5\Phi_h\upsilon_r + \upsilon_h p_h(1-\psi)\upsilon_r\sigma_3\sigma_5\Phi_h\upsilon_r\left(\mathcal{R}_0^r - 1\right) + \upsilon_h p_h(1-\psi)\upsilon_r\sigma_3\sigma_5\Phi_h\upsilon_r\\
&+ \tau p_h(1-\psi)\upsilon_r\sigma_3\sigma_5\Phi_h\upsilon_r\left(\mathcal{R}_0^r - 1\right) + \tau p_h(1-\psi)\upsilon_r\sigma_3\sigma_5\Phi_h\upsilon_r + \gamma p_h(1-\psi)\upsilon_r\sigma_3\sigma_5\Phi_h\upsilon_r\left(\mathcal{R}_0^r - 1\right)\\
&+ \gamma p_h(1-\psi)\upsilon_r\sigma_3\sigma_5\Phi_h\upsilon_r + p_h\psi p_h(1-\psi)\upsilon_r\sigma_3\sigma_5\Phi_h\upsilon_r\left(\mathcal{R}_0^r - 1\right) + p_h\psi p_h(1-\psi)\upsilon_r\sigma_3\sigma_5\Phi_h\upsilon_r\\
&- (1-\chi)\varrho_h p_h(1-\psi)\sigma_3\sigma_5\upsilon_h\upsilon_r\Phi_h\upsilon_r\left(\mathcal{R}_0^r - 1\right) - (1-\chi)\varrho_h\alpha\sigma_2\sigma_3\sigma_4 p_r\upsilon_h\Phi_h\upsilon_r\left(\mathcal{R}_0^r - 1\right),\\
A_2 =&\upsilon_r\left(\mathcal{R}_0^r - 1\right)\sigma_4\sigma_2\left(\sigma_1\sigma_3 - \vartheta\varpi\right)\left(1 - \mathcal{R}_c^h\right).
\end{aligned} \tag{3.70}$$

Equation (3.67) can be solved to get

$$\phi^{**} = \frac{A_2}{A_1}. \tag{3.71}$$

Hence, A_2 becomes

$$A_2 = \upsilon_r\left(\mathcal{R}_0^r - 1\right)\sigma_4\sigma_2\left(\sigma_1\sigma_3 - \vartheta\varpi\right)\left(\mathcal{R}_c^h - 1\right). \tag{3.72}$$

Hence, the result follows.

Theorem 3.7. *Model* (2.1) *possesses a unique endemic equilibrium if* $\mathcal{R}_0^r > 1$ *and* $\mathcal{R}_c^h > 1$ *or if* $\mathcal{R}_c > 1$.

3.10. Global stability of endemic equilibrium point: a special case

Setting $\vartheta = \mu = \gamma = \psi = 0$ in model (2.1), we have

$$\begin{aligned}
\frac{dS_h}{dt} &= \Phi_h - \phi_h S_h - (\upsilon_h + \varpi)S_h,\\
\frac{dE_h}{dt} &= \phi_h S_h - (p_h + \upsilon_h + \mu)E_h,\\
\frac{dV_h}{dt} &= \varpi S_h - (\upsilon_h + \gamma)V_h,\\
\frac{dI_h}{dt} &= p_h E_h - (\upsilon_h + \delta_h + \tau)I_h,\\
\frac{dR_h}{dt} &= \tau I_h - \upsilon_h R_h,\\
\frac{dS_r}{dt} &= \Phi_r - \phi_r S_r - \upsilon_r S_r,\\
\frac{dE_r}{dt} &= \phi_r S_r - (p_r + \upsilon_r)E_r,\\
\frac{dI_r}{dt} &= p_r E_r - \upsilon_r I_r.
\end{aligned} \tag{3.73}$$

Theorem 3.8. *Suppose the vaccine waning rate (ϑ), post-exposure vaccination rate (μ), immunity rate (γ), and early therapeutic education (ψ) are all neglected, and the endemic equilibrium is globally asymptotically stable if $\mathcal{R}_c^h > 1$ and $\mathcal{R}_c^{\mathcal{R}} > 1$. Otherwise, if $\mathcal{R}^c > 1$, it is unstable.*

Proof. Let V be a Lyapunov function of the Goh-Volterra form, constructed as

$$\begin{aligned}
V = &\left(S_h - S_h^{**} - S_h^{**}\ln\frac{S_h}{S_h^{**}}\right) + \left(E_h - E_h^{**} - E_h^{**}\ln\frac{E_h}{E_h^{**}}\right) + \left(V_h - V_h^{**} - V_h^{**}\ln\frac{V_h}{V_h^{**}}\right)\\
&+ \frac{p_h + \upsilon_h + \mu}{p_h}\left(I_h - I_h^{**} - I_h^{**}\ln\frac{I_h}{I_h^{**}}\right) + \frac{(p_h + \upsilon_h + \mu)(\upsilon_h + \delta_h + \tau)}{p_h\tau}\left(R_h - R_h^{**} - R_h^{**}\ln\frac{R_h}{R_h^{**}}\right)\\
&+ \left(S_r - S_r^{**} - S_r^{**}\ln\frac{S_r}{S_r^{**}}\right) + \left(E_r - E_r^{**} - E_r^{**}\ln\frac{E_r}{E_r^{**}}\right) + \frac{p_r + \upsilon_r}{p_r}\left(I_r - I_r^{**} - I_r^{**}\ln\frac{I_r}{I_r^{**}}\right).
\end{aligned} \tag{3.74}$$

Differentiating V with respect to time yields

$$\begin{aligned}
\dot{V} = &\left(1 - \frac{S_h^{**}}{S_h}\right)\dot{S}_h + \left(1 - \frac{E_h^{**}}{E_h}\right)\dot{E}_h + \left(1 - \frac{V_h^{**}}{V_h}\right)\dot{V}_h + \frac{p_h + \upsilon_h + \mu}{p_h}\left(1 - \frac{I_h^{**}}{I_h}\right)\dot{I}_h\\
&+ \frac{(p_h + \upsilon_h + \mu)(\upsilon_h + \delta_h + \tau)}{p_h\tau}\left(1 - \frac{R_h^{**}}{R_h}\right)\dot{R}_h + \left(1 - \frac{S_r^{**}}{S_r}\right)\dot{S}_r + \left(1 - \frac{E_r^{**}}{E_r}\right)\dot{E}_r\\
&+ \frac{p_r + \upsilon_r + \mu}{p_r}\left(1 - \frac{I_r^{**}}{I_r}\right)\dot{I}_r.
\end{aligned} \tag{3.75}$$

Substituting model (3.73) into Eq (3.75) leads to:

$$\begin{aligned}\dot{V} &= \left(1-\frac{S_h^{**}}{S_h}\right)(\Phi_h-\phi_h S_h-(\upsilon_h+\varpi)S_h)+\left(1-\frac{E_h^{**}}{E_h}\right)(\phi_h S_h-(p_h+\upsilon_h+\mu)E_h)\\ &+\left(1-\frac{V_h^{**}}{V_h}\right)(\varpi S_h-(\upsilon_h+\gamma)V_h)+\frac{p_h+\upsilon_h+\mu}{p_h}\left(1-\frac{I_h^{**}}{I_h}\right)(p_hE_h-(\upsilon_h+\delta_h+\tau)I_h)\\ &+\frac{(p_h+\upsilon_h+\mu)(\upsilon_h+\delta_h+\tau)}{p_h\tau}\left(1-\frac{R_h^{**}}{R_h}\right)(\tau I_h-\upsilon_h R_h)+\left(1-\frac{S_r^{**}}{S_r}\right)(\Phi_r-\phi_r S_r-\upsilon_r S_r)\\ &+\left(1-\frac{E_r^{**}}{E_r}\right)(\phi_r S_r-(p_r+\upsilon_r)E_r)+\frac{p_r+\upsilon_r+\mu}{p_r}\left(1-\frac{I_r^{**}}{I_r}\right)(p_rE_r-\upsilon_r I_r)\,.\end{aligned} \tag{3.76}$$

The equilibrium conditions are

$$\begin{aligned}\Phi_h &= \phi_h S_h^{**}+\upsilon_h S_h^{**},\\ \Phi_r &= \phi_r S_r^{**}+\upsilon_r S_r^{**},\\ (p_h+\upsilon_h+\mu)E_h^{**} &= \phi_h S_h^{**},\\ \varpi S_h^{**} &= \upsilon_h V_h^{**},\\ (\upsilon_h+\delta_h+\tau)I_h^{**} &= p_h E_h^{**},\\ \upsilon_h R_h^{**} &= \tau I_h^{**},\\ (p_r+\upsilon_r)E_r^{**} &= \phi_r S_r^{**},\\ \upsilon_r I_r^{**} &= p_r E_r^{**}.\end{aligned} \tag{3.77}$$

Substituting (3.77) into (3.76) and we obtain

$$\begin{aligned}\dot{V} &\le (\upsilon_h+\varpi)S_h^{**}\left(2-\frac{S_h}{S_h^{**}}-\frac{S_h^{**}}{S_h}\right)+\upsilon_h V_h^{**}\left(2-\frac{V_h}{V_h^{**}}-\frac{V_h^{**}}{V_h}\right)\\ &+\phi_h S_h^{**}\left(5-\frac{S_h^{**}}{S_h}-\frac{S_hE_h^{**}}{S_h^{**}E_h}-\frac{E_hI_h^{**}}{E_h^{**}I_h}-\frac{R_h}{R_h^{**}}-\frac{I_hR_h^{**}}{I_h^{**}R_h}\right)\\ &+\upsilon_r S_r^{**}\left(2-\frac{S_r}{S_r^{**}}-\frac{S_r^{**}}{S_r}\right)+\phi_r S_r^{**}\left(3-\frac{S_r}{S_r^{**}}-\frac{S_rE_r^{**}}{S_r^{**}E_r}-\frac{I_r^{**}}{I_r}\right).\end{aligned} \tag{3.78}$$

Applying the arithmetic–geometric mean inequality to each term confirm the following:

$$\begin{aligned}&\left(2-\frac{S_h}{S_h^{**}}-\frac{S_h^{**}}{S_h}\right)\le 0,\left(2-\frac{V_h}{V_h^{**}}-\frac{V_h^{**}}{V_h}\right)\le 0,\left(5-\frac{S_h^{**}}{S_h}-\frac{S_hE_h^{**}}{S_h^{**}E_h}-\frac{E_hI_h^{**}}{E_h^{**}I_h}-\frac{R_h}{R_h^{**}}-\frac{I_hR_h^{**}}{I_h^{**}R_h}\right)\le 0\\ &\left(2-\frac{S_r}{S_r^{**}}-\frac{S_r^{**}}{S_r}\right)\le 0,\left(3-\frac{S_r}{S_r^{**}}-\frac{S_rE_r^{**}}{S_r^{**}E_r}-\frac{I_r^{**}}{I_r},\right)\le 0,\end{aligned} \tag{3.79}$$

which will lead to $\dot{V}\le 0$, provided that $\vartheta=\mu=\gamma=\psi=0$ and $\mathcal{R}_c^h>1, \mathcal{R}_0^r>1$, that is, $\mathcal{R}_c>1$.

Since all relevant compartments—$S_h, E_h, V_h, I_h, R_h, S_r, E_r, I_r$—are at endemic equilibrium, it follows from model (3.73) that:

$$\lim_{t\to\infty}(S_h(t),E_h(t),V_h(t),I_h(t),R_h(t),S_r(t),E_r(t),I_r(t))\to(S_h^{**},E_h^{**},V_h^{**},I_h^{**},R_h^{**},S_r^{**},E_r^{**},I_r^{**}).$$

Therefore, by invoking LaSalle's invariance principle [39–41], the endemic equilibrium is globally asymptotically stable (GAS) [31].

Theorem 3.8 thus demonstrates that the endemic equilibrium persists and remains stable under the condition $\mathcal{R}_c > 1$, when vaccine waning rate (ϑ), post-exposure vaccination rate (μ), immunity rate (γ), and early therapeutic education (ψ) are negligible. □

4. Data fittings

The source (publicly accessible Mpox surveillance data), time duration, population taken into consideration, and preprocessing procedures (such as smoothing, normalization, and treatment of missing values) of the epidemiological data utilized for model calibration are all fully described. We explicitly describe the method used for parameter estimate. Using a nonlinear least-squares optimization framework, the model's cumulative (or incidence) infected instances were fitted to observed data in order to estimate the model's parameters. Standard numerical solvers were used to optimize the fitting process, which minimizes the sum of squared discrepancies between model predictions and observed data. We now present suitable goodness-of-fit metrics to test model performance, such as the root-mean-square error (RMSE) and coefficient of determination (R^2), which show how well the model captures observed Mpox dynamics. By calculating confidence intervals using a bootstrap/Latin hypercube sampling-based method, we have integrated uncertainty quantification for the calculated parameters. The resulting uncertainty bounds, which shed light on the robustness of model predictions and parameter identifiability, are presented and debated.

Validating models and accurately determining parameter values are crucial challenges in the field of MD with empirical data. This is because parameter values are frequently not directly obtained from the data that has been gathered. Consequently, estimating the parameters for the specified model becomes crucial. Certain parameters can be easily approximated by considering the early dynamics of an epidemic in conjunction with the disease-related demographic characteristics. Furthermore, parameters values can be obtained from the body of existing research, which can be used as estimation benchmarks, but depending only on values drawn from literature can occasionally result in unanticipated results. These real-world examples can cover a range of time periods, from days to years, and the results could be impacted by errors introduced during data processing. The least-squares approach is the most widely used method for parameter estimation, even though there are many other approaches available in the literature.

Although many epidemiological models have been identified and validated, parameter estimation is still a major challenge. The parameters of the suggested model are estimated using empirical data and kept within acceptable boundaries to guarantee that it appropriately depicts the Mpox virus. Importantly, instead of using values from existing Mpox models in the literature, parameter estimation makes it easier to obtain values unique to the established model. The least-squares curve fitting method was used to estimate the relevant parameters using patient data. For a least-squares fit to the model parameters, data from the Nigeria's CDC dashboard covering 12 months (May 29, 2022–May 21, 2023), as cited in [39], were used. By reducing the sum of squared errors (SSE) between the model's solution for infectious HUMs and the real Mpox data, the ideal parameter values were found. The biological parameters of the model and their ideal values are listed in Table 1. Figure 2 exhibits the actual values as solid blue circles and the best-fitting model curve as a solid orange line, displaying

a strong agreement between the fitted curve and the empirical data, thus verifying the model, while Figure 3 shows the residuals. Additionally, there are no outliers in the statistical case summary shown in Figure 4, and the most significant statistical case summaries are summarized in Table 3, all of which are consistent. Nigeria's monkey-pox virus weekly data (week 1–52) from May 29, 2022, to May 21, 2023 is given in Table 4.

The following shows how the least-squares method minimizes the residuals between the discrete points derived from the simulation of the proposed equations $h(t_j, x_j)$ and the observed infection data $\hat{x}_j = 0, 1, ..., n$:

$$\text{Residual} = \frac{1}{N}\sum_{j=0}^{N}\left|\frac{\hat{x}_j - x_j}{\hat{x}_j}\right|. \tag{4.1}$$

This goal was accomplished by estimating the precise parameters of the ordinary differential equation (ODE) system for the given dataset using curve fitting and the built-in scipy algorithms for ODE systems in Python 3.12.1. The following initial conditions were applied while estimating the parameters:

$$\begin{aligned} &S_h(0) = 112,617,070, E_h(0) = 1300, V_h(0) = 51,180,820, I_h(0) = 810, R_h(0) = 60,000,000, \\ &S_r(0) = 170,000,000, E_r(0) = 600,000, I_r(0) = 90,000. \end{aligned} \tag{4.2}$$

Table 3. Summary statistics for real and predicted data.

Statistics	Min	Q1	Q2 (Median)	Q3	Mean	Max	Standard Deviation
Real	25	860	585	690	480	850	270
Predicted	875	650	670	660	464	860	260

Table 4. Nigeria's monkey-pox virus weekly data (week 1–52) from May 29, 2022, to May 21, 2023 [39].

Period	Number of confirmed cases	Cumulative confirmed cases
May 29-June 30	25	25
July 1-July 31	70	95
August 1-August 31	59	154
September 1-September 30	146	300
October 1-October 30	138	438
November 1- November 30	147	585
December 1- December 31	54	639
January 1- January 31	70	709
February 1- February 28	30	739
March 1- March 31	30	769
April 1-April 30	20	789
May 1-May 21	21	810

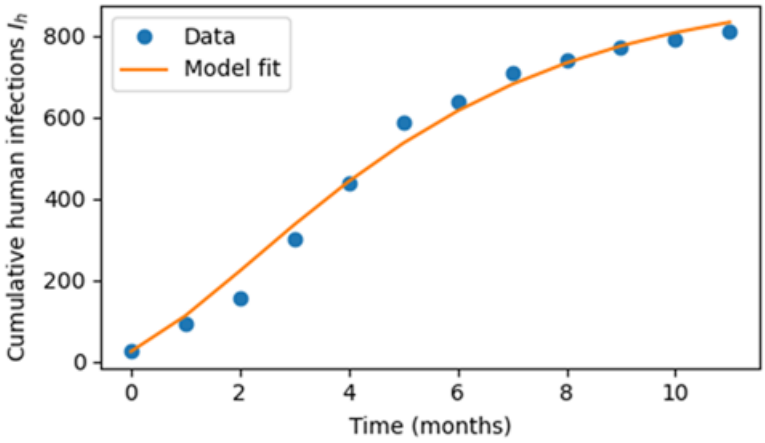

Figure 2. Comparison between observed Mpox case data and model-generated simulation results.

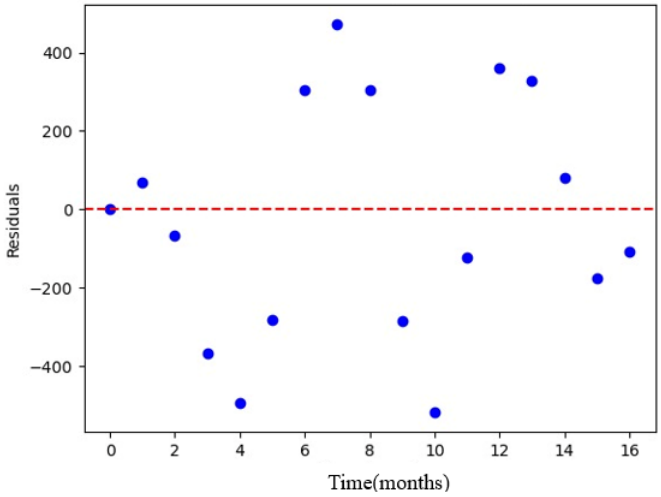

Figure 3. Residual plot illustrating the performance of the least-squares fitting applied to the proposed model.

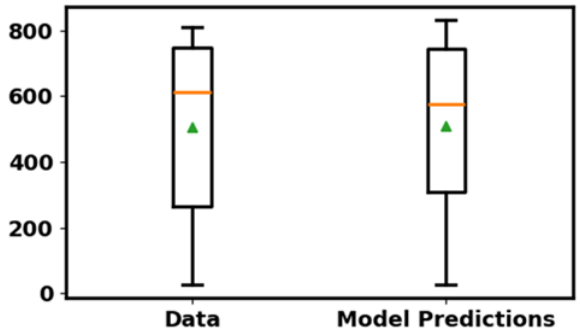

Figure 4. Statistical illustration of the real data and the model's predicted values via a box and whisker plot.

4.1. Sensitivity analysis

We carried out uncertainty and sensitivity analysis of the model parameters employing Latin hypercube sampling (LHS) and partial rank correlation coefficient (PRCC). For the purpose of producing the LHS matrices, we assumed that the entire model parameters are uniformly distributed. A total of $1,000$ simulations of the model per LHS parameters were performed, by means of the baseline values in Table 1. Figures 5 and 6 illustrate the PRCC values for: (i) HUM-related parameters, and (ii) rodents-related parameters using the monkey pox control reproduction number $\mathbb{R}_c$ as the response function. The PRCC results are tabulated in Table 5 below.

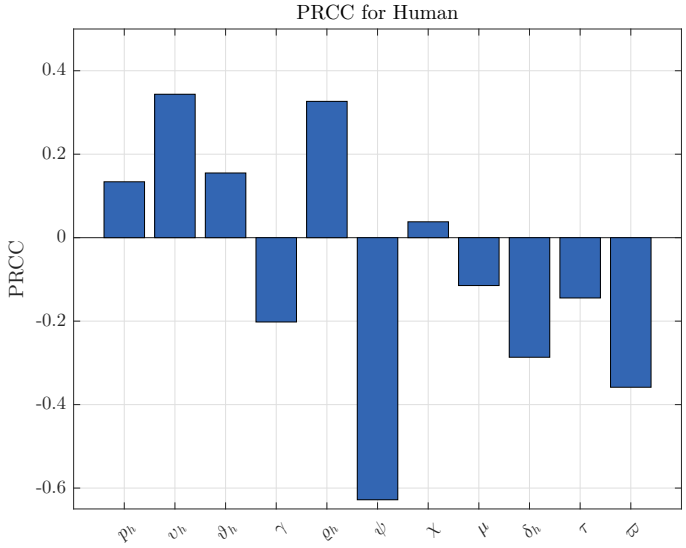

Figure 5. Figure showing the PRCC values of R_c^h.

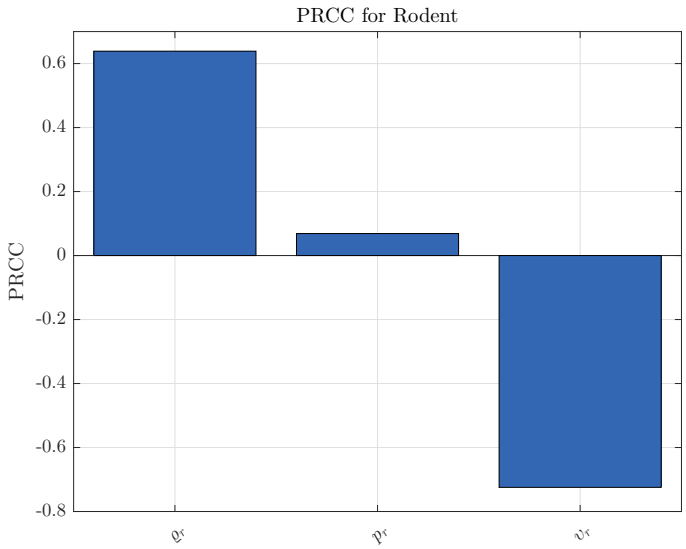

Figure 6. Figure showing the PRCC values of R_c^r.

Table 5. PRCC values for the parameters of model (2.1) using R_c as response function with all parameter values used shown in Table 1.

Parameter	PRCC Value of R_c
p_h	0.0457
ϑ_h	0.2161
υ_h	0.3478
γ	−0.1557
ϱ_h	0.3682
ψ	−0.6434
χ	−0.0457
μ	−0.1182
δ_h	−0.2829
τ	−0.1419
ϖ	−0.4071
ϱ_r	0.6388
p_r	0.0688
υ_r	−0.7246

Figure 7 is a contour diagram of the HUM control reproduction number $\mathcal{R}_c^h$ with respect to variations in χ and ψ. Figure 8 is a contour diagram of the HUM control reproduction number $\mathcal{R}_c^h$ with respect to variations in ϑ and δ_h. Figure 9 is a contour diagram of the HUM control reproduction number $\mathcal{R}_c^h$ with respect to variations in γ and μ. Figure 10 is a contour diagram of the HUM control reproduction number $\mathcal{R}_c^h$ with respect to variations in τ and ψ. Figure 11 reveals that higher values of the host mortality (δ_h) and natural death rate (μ) are associated with a lower $\mathcal{R}_c$, emphasizing the dampening effect of host turnover on transmission dynamics. Figure 12 shows that $\mathcal{R}_c$ increases with both p_h and ϑ_h, implying that higher host infection or transmission probabilities enhance epidemic intensity. Figure 13 highlights that both ψ and ϖ exert a strong negative influence on $\mathcal{R}_c$, confirming that control and intervention parameters are effective in reducing the basic reproduction number. Conversely, Figure 14 demonstrates that $\mathcal{R}_c$ declines gradually with increasing v_h, indicating that improved vector mortality or control reduces disease persistence. Figure 15 illustrates a strong positive association between $\mathcal{R}_c$ and the parameters ρ_r and p_r, indicating that increases in either the contact rate or transmission probability in the reservoir population lead to higher transmission potential. In Figure 16, $\mathcal{R}_c$ similarly rises with ρ_r but exhibits a weaker sensitivity to υ_r, suggesting that variations in the recovery or removal rate of the reservoir have a comparatively minor influence. Collectively, these results indicate that transmission-related parameters ($\upsilon_h, \varrho_h, \varrho_r$) act as key amplifiers of infection spread, whereas mortality, recovery, and control parameters ($\upsilon_r, \delta_h, \mu, \psi, \varpi$) play a stabilizing role by diminishing $\mathcal{R}_c$.

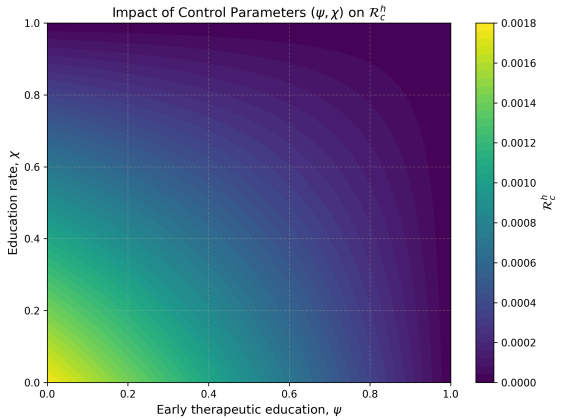

Figure 7. Contour diagram of the HUM control reproduction number $\mathcal{R}_c^h$ with respect to variations in χ and ψ.

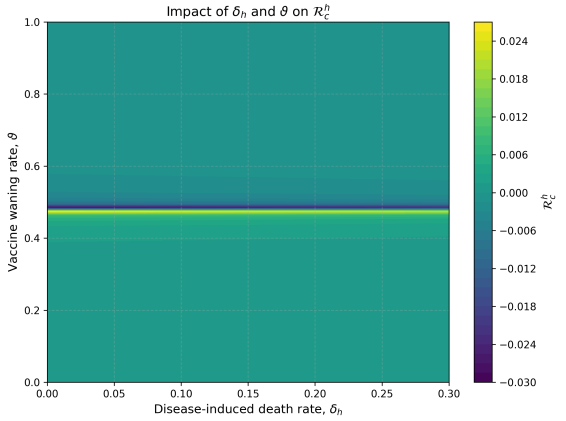

Figure 8. Contour diagram of the HUM control reproduction number $\mathcal{R}_c^h$ with respect to variations in ϑ and δ_h.

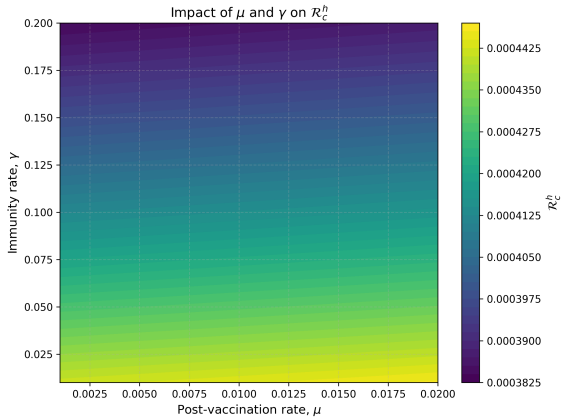

Figure 9. Contour diagram of the HUM control reproduction number $\mathcal{R}_c^h$ with respect to variations in γ and μ.

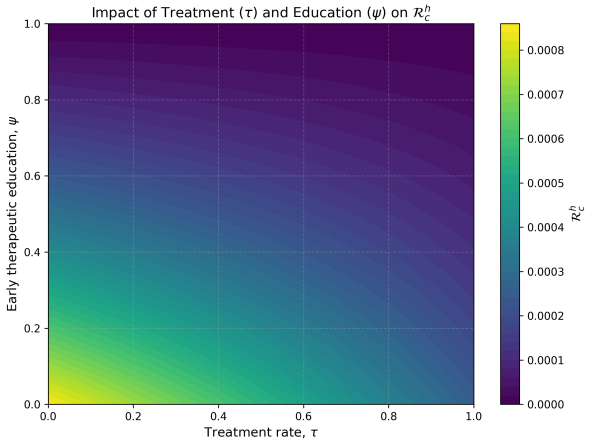

Figure 10. Contour diagram of the HUM control reproduction number $\mathcal{R}_c^h$ with respect to variations in τ and ψ.

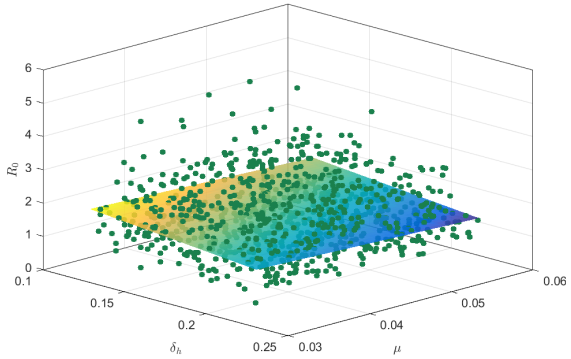

Figure 11. 3D plot showing the effect of δ_h and μ on $\mathcal{R}_c$.

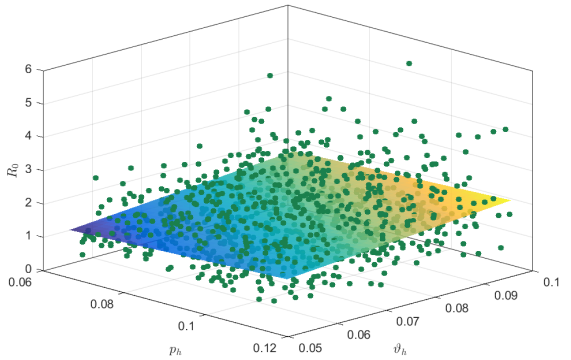

Figure 12. 3D plot showing the effect of p_h and ϑ_h on $\mathcal{R}_c$.

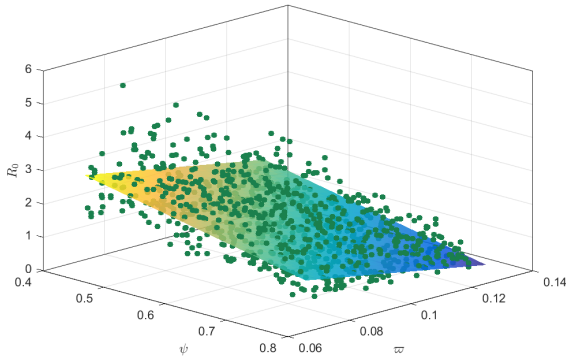

Figure 13. 3D plot showing the effect of ψ and ϖ on $\mathcal{R}_c$.

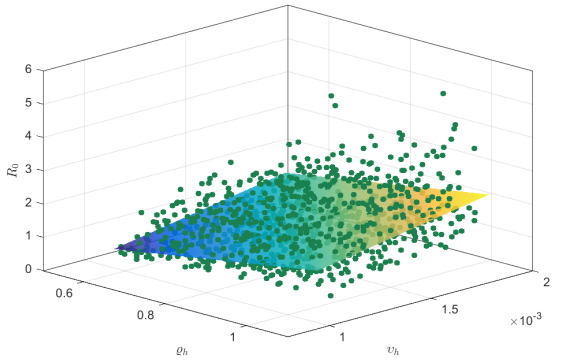

Figure 14. 3D plot showing the effect of ϱ_h and υ_h on $\mathcal{R}_c$.

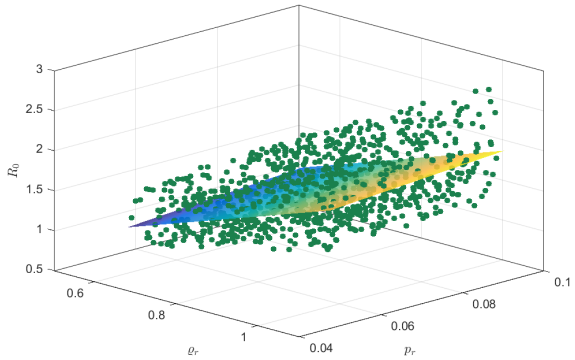

Figure 15. 3D plot showing the effect of ϱ_r and p_r on $\mathcal{R}_c$.

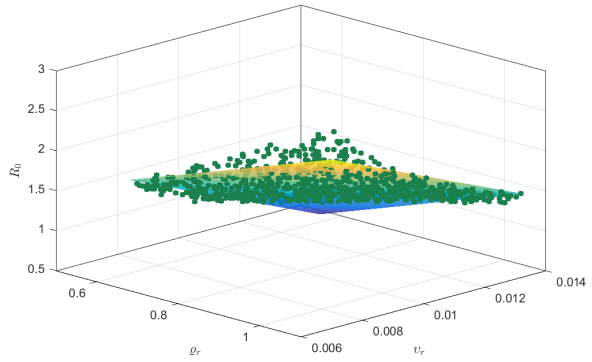

Figure 16. 3D plot showing the effect of ϱ_r and υ_{hr} on $\mathcal{R}_c$.

5. Numerical simulations

This section presents a qualitative simulation of model (2.1) using MATLAB 2024a, with the values in Table 1. In some cases, the values of certain parameters were increased to ensure the reproduction number exceeded unity, and these are specified in the relevant figures.

5.1. Discussion of the simulated figures

Figure 17a illustrates the cumulative cases of Mpox. When the presence of education is included in the HUM population, we noticed that when the education rate varies or increases, the cases reduce to a minimum. Also, it was noted that if education about the disease is perfect, the disease goes extinct. Figure 17b illustrates the cumulative cases of Mpox. When there is imperfect vaccination in the HUM population, we noticed that when the imperfect vaccination rate varies or increases, the cases reduce, but not to a minimum. Also, it was noted that if the imperfect vaccination against the disease is 5%, the imperfect vaccination helped to some extent. Figure 17c illustrates the cumulative cases of Mpox. When there is education in the HUM population, we noticed that when the education rate varies or increases, the cases reduce to a minimum (that is, the disease is wiped out from the environment; note that $\mathcal{R}_c^h = 1.7981$ and $\mathcal{R}_0^r = 9.091$, when $\varrho_h = 0.9$, $\varpi = 0.000058$, and $p_h = 0.989$). Also, it was noted that if education about the disease is made perfect, the disease goes extinct. Figure 17d illustrates the cumulative cases of Mpox. When there is imperfect vaccination in the HUM population, we noticed that when the imperfect vaccination rate varies or increases, the cases reduce (that is, the disease reduces from the environment; note that $\mathcal{R}_c^h = 1.7981$ and $\mathcal{R}_0^r = 9.091$, when $\varrho_h = 0.9$, $\varpi = 0.000058$, and $p_h = 0.989$), but not to a minimum. Also, it was noted that if the imperfect vaccination against the disease is 5%, it helped to reduce the disease to some extent.

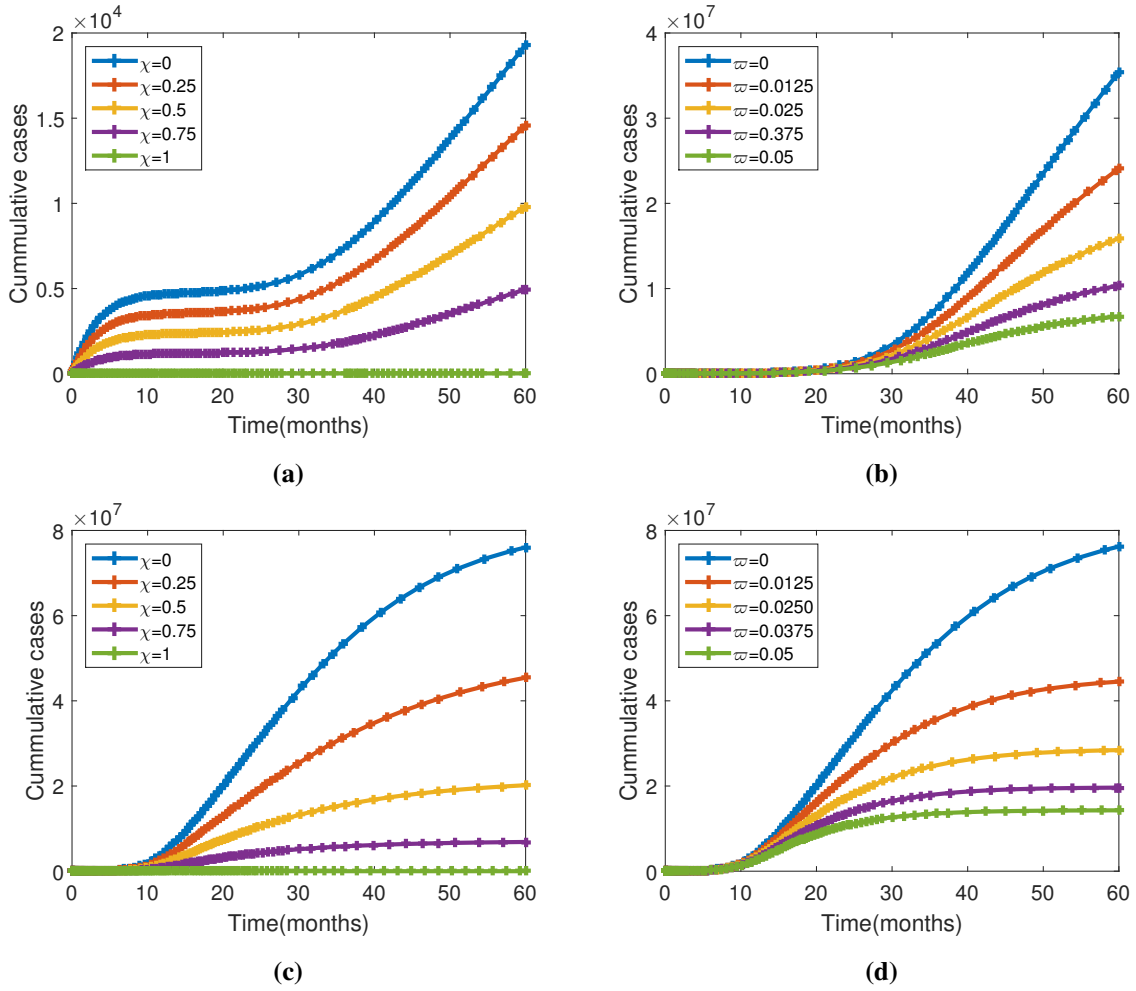

Figure 17. Figure demonstrating (**a**) the cumulative cases of Mpox varying education rate at $\mathcal{R}_c^h < 1$ and $\mathcal{R}_0^r < 1$, (**b**) the cumulative cases of Mpox varying imperfect vaccination rate at $\mathcal{R}_c^h < 1$ and $\mathcal{R}_0^r < 1$, (**c**) the cumulative cases of Mpox varying education rate at $\mathcal{R}_c^h = 1.7981$ and $\mathcal{R}_0^r = 9.091$, when $\varrho_h = 0.9$, $\varpi = 0.000058$, and $p_h = 0.989$, and (**d**) the cumulative cases of Mpox varying imperfect vaccination rate at $\mathcal{R}_c^h = 1.7981$ and $\mathcal{R}_0^r = 9.091$, when $\varrho_h = 0.9$, $\varpi = 0.000058$, and $p_h = 0.989$.

Figure 18a illustrates the impact of imperfect vaccination on susceptible HUMs. When there is imperfect vaccination in the HUM population, we noticed that when the imperfect vaccination rate varies or increases, the susceptible HUMs increase immensely over time. Also, it was noted that if the imperfect vaccination against the disease is increased to 5%, the susceptible individuals grow over time; this result may be due to the failure of imperfect vaccination. Figure 18b illustrates the cumulative cases of Mpox. When there is post-exposure vaccination in the HUM population, we noticed that when the post-exposure vaccination rate varies or increases, the cases reduce, but not to a minimum. Also, it was noted that if 100% of the exposed HUMs have a post-exposure vaccination against the disease, it can help to some extent. Figure 19a illustrates the impact of education on exposed HUMs. When there is education in the HUM population, we noticed when the education rate varies or increases, it increases around the 14–18th weeks, and the cases reduce to a minimum (that is, the

population of exposed HUMs reduces to zero, or it wipes out the population from the environment; note that $\mathcal{R}_c^h < 1$ and $\mathcal{R}_0^r < 1$). Also, it was noted that if education about the disease is perfect, the disease goes extinct. Figure 19b illustrates the impact of education on exposed HUMs. When there is education in the HUM population, we noticed when the education rate varies or increases, the cases increase immensely around the 10–20th weeks, and the cases reduce to a minimum after that (that is, the population of exposed HUMs reduces to zero, or it wiped out the population from the environment; note that $\mathcal{R}_c^h = 1.7981$ and $\mathcal{R}_0^r = 9.091$, when $\varrho_h = 0.9$, $\varpi = 0.000058$, and $p_h = 0.989$). Also, it was noted that if education about the disease is perfect, the disease goes extinct.

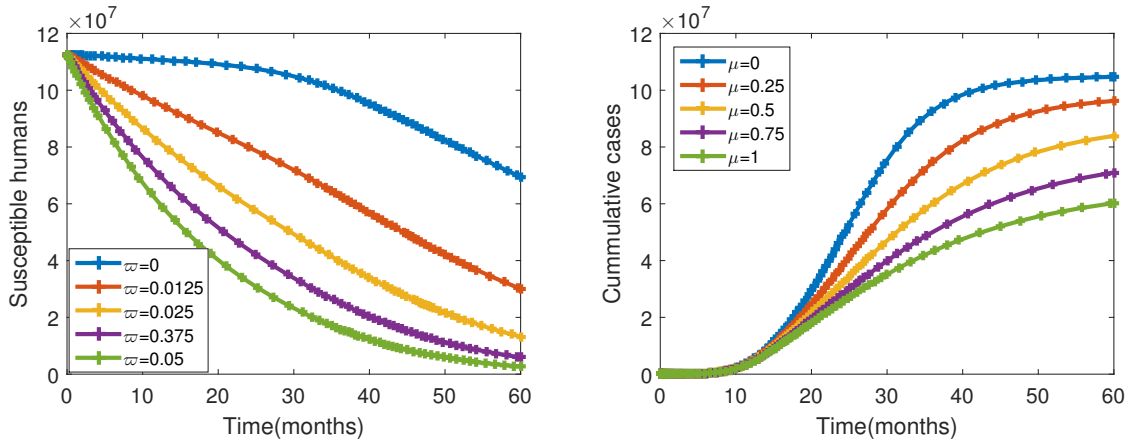

(a) **(b)**

Figure 18. Figure demonstrating (**a**) the effect of imperfect vaccination on susceptible HUMs, varying the imperfect vaccination rate, and (**b**) the cumulative cases of Mpox varying post-exposure vaccination rate at $\mathcal{R}_c^h = 1.7981$ and $\mathcal{R}_0^r = 9.091$, when $\varrho_h = 0.9$, $\varpi = 0.000058$, and $p_h = 0.989$.

Figure 19c illustrates the impact of education on infectious HUMs. When there is education in the HUM population, we noticed when the education rate varies or increases around the 24–28th weeks, the cases reduce to a minimum (that is, the population of infectious HUMs reduces to zero, or it wiped out the infectious population from the environment; note that $\mathcal{R}_c^h < 1$ and $\mathcal{R}_0^r < 1$). Also, it was noted that if education about the disease is perfect, the infectious HUM population goes extinct. Figure 19d illustrates the impact of education on infectious diseases. When there is education in the HUM population, we noticed when education rate varies or increases, the cases increase immensely around the 20–25th weeks, and the cases reduce to a minimum after that (that is, the population of infectious HUMs reduces to zero, or it wiped out the population from the environment; note that $\mathcal{R}_c^h = 1.7981$ and $\mathcal{R}_0^r = 9.091$, when $\varrho_h = 0.9$, $\varpi = 0.000058$, and $p_h = 0.989$). Also, it was noted that if education about the disease is perfect, the infectious HUMs will go extinct. Figure 20a illustrates the impact of education on susceptible HUMs. When there is education in the HUM population, we noticed that when the education rate varies or increases, the susceptible HUMs increase over time. Also, it was noticed that if education against the disease is increased to almost perfect, the susceptible individuals grow over time. Figure 20b illustrates the impact of education on vaccinated HUMs. When there is education in the HUM population, we noticed that when the education rate varies or increases, the susceptible HUMs increase (that is, the population of vaccinated HUMs reduces to zero; note that

$\mathcal{R}_c^h = 1.7981$ and $\mathcal{R}_0^r = 9.091$, when $\varrho_h = 0.9$, $\varpi = 0.000058$, and $p_h = 0.989$).

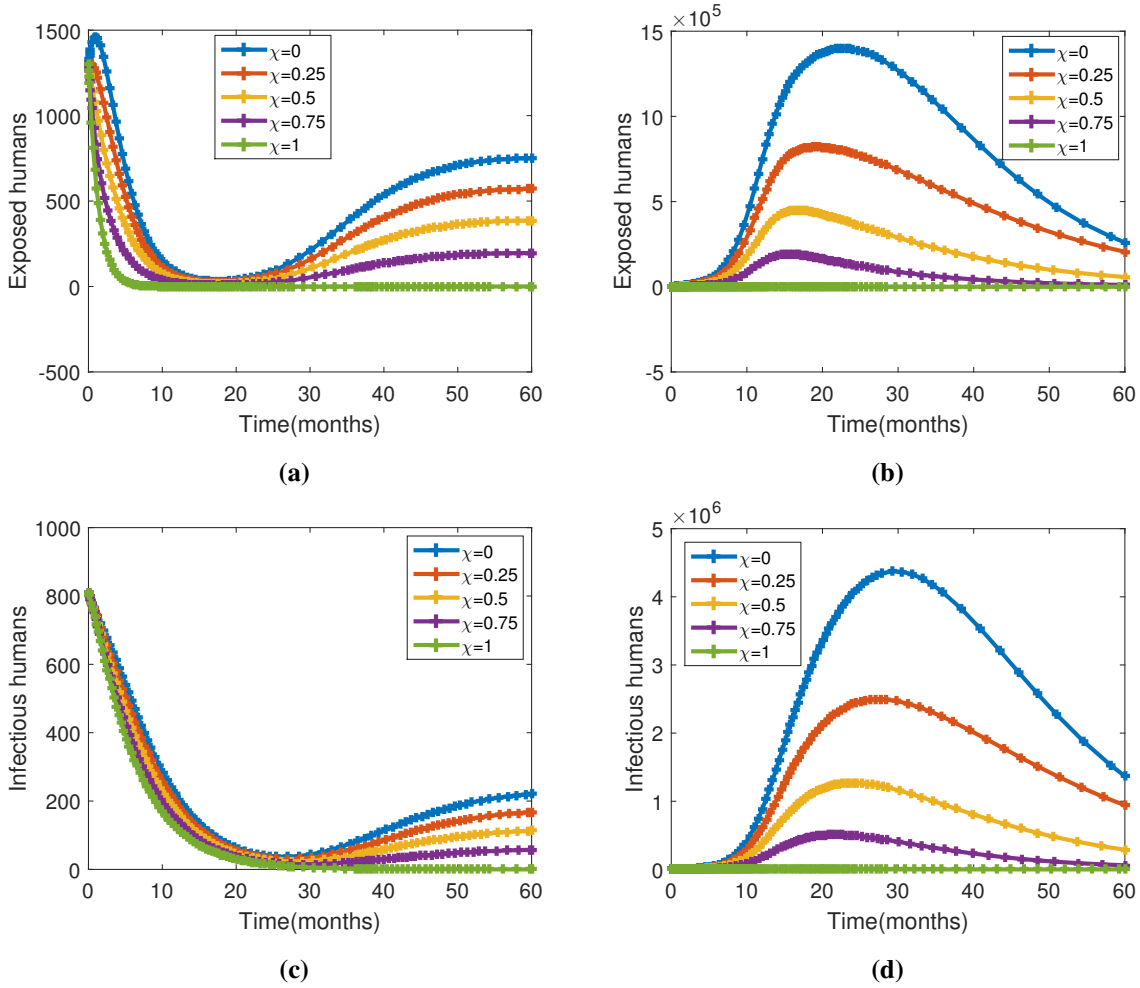

Figure 19. Figure demonstrating (**a**) the effect of education on exposed HUMs, varying education rate at $\mathcal{R}_c^h < 1$ and $\mathcal{R}_0^r < 1$, (**b**) the effect of education on exposed HUMs while $\mathcal{R}_c^h = 1.7981$ and $\mathcal{R}_0^r = 9.091$, when $\varrho_h = 0.9$, $\varpi = 0.000058$, and $p_h = 0.989$, (**c**) the effect of education on infectious HUMs, varying education rate at $\mathcal{R}_c^h < 1$ and $\mathcal{R}_0^r < 1$, and (**d**) the effect of education on infectious HUMs while $\mathcal{R}_c^h = 1.7981$ and $\mathcal{R}_0^r = 9.091$, when $\varrho_h = 0.9$, $\varpi = 0.000058$, and $p_h = 0.989$.

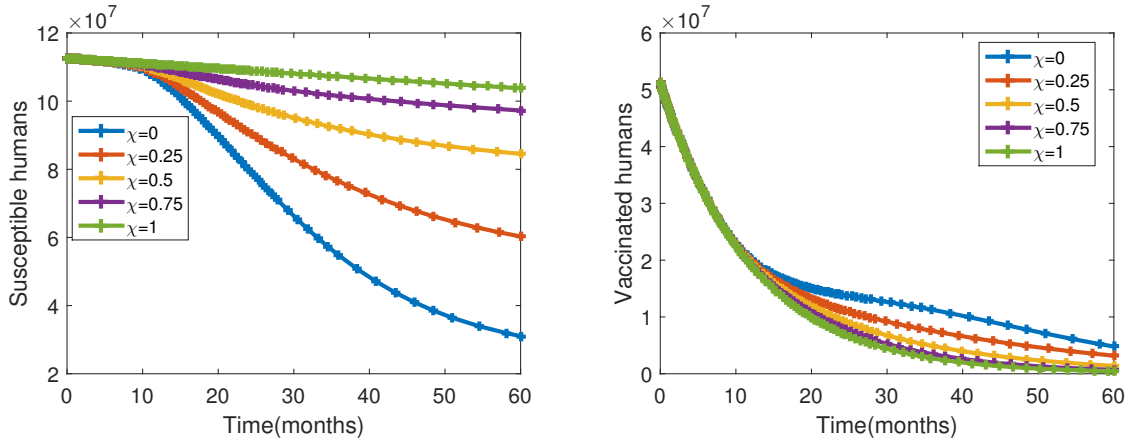

(a) **(b)**

Figure 20. Figure demonstrating (**a**) the effect of education on susceptible HUMs, varying the education rate at $\mathcal{R}_c^h = 1.7981$ and $\mathcal{R}_0^r = 9.091$, when $\varrho_h = 0.9$, $\varpi = 0.000058$, and $p_h = 0.989$, and (**b**) the effect of education on vaccinated HUMs, varying the education rate at $\mathcal{R}_c^h = 1.7981$ and $\mathcal{R}_0^r = 9.091$, when $\varrho_h = 0.9$, $\varpi = 0.000058$, and $p_h = 0.989$.

Figure 21a illustrates the impact of post-exposure vaccination on exposed HUMs. When there is post-exposure vaccination in the HUM population, we noticed that when the post-exposure vaccination rate varies or increases, that is it decreases around the 5-20th weeks, and the cases increase after that to some extent (that is, the population of exposed HUMs increases; note that $\mathcal{R}_c^h < 1$ and $\mathcal{R}_0^r < 1$). Figure 21b illustrates the impact of post-exposure vaccination on exposed HUMs. When there is post-exposure vaccination control in the HUM population, we noticed that when the post-exposure vaccination rate varies or increases, the cases increase immensely around the 10–20th weeks, and the cases reduce to a minimum after that (that is, the population of exposed HUMs reduces to zero, or it wiped out the population from the environment; note that $\mathcal{R}_c^h = 1.7981$ and $\mathcal{R}_0^r = 9.091$, when $\varrho_h = 0.9$, $\varpi = 0.000058$, and $p_h = 0.989$). Figure 21c illustrates the impact of post-exposure vaccination on infectious HUMs. When there is post-exposure vaccination in the HUM population, we noticed that when the post-exposure vaccination rate varies or increases, it decreases around the 5–20th weeks and the infectious HUMs increases after that, to some extent (that is, the population of exposed HUMs increases; note that $\mathcal{R}_c^h < 1$ and $\mathcal{R}_0^r < 1$). Figure 21d illustrates the impact of post-exposure vaccination on infectious HUMs. When there is post-exposure vaccination in the HUM population, we noticed that when the post-exposure vaccination rate varies or increases, the cases increase immensely around the 20–25th weeks, and the cases reduce to a minimum after that (that is, the population of infectious HUMs reduces to minimum; note that $\mathcal{R}_c^h = 1.7981$ and $\mathcal{R}_0^r = 9.091$, when $\varrho_h = 0.9$, $\varpi = 0.000058$, and $p_h = 0.989$).

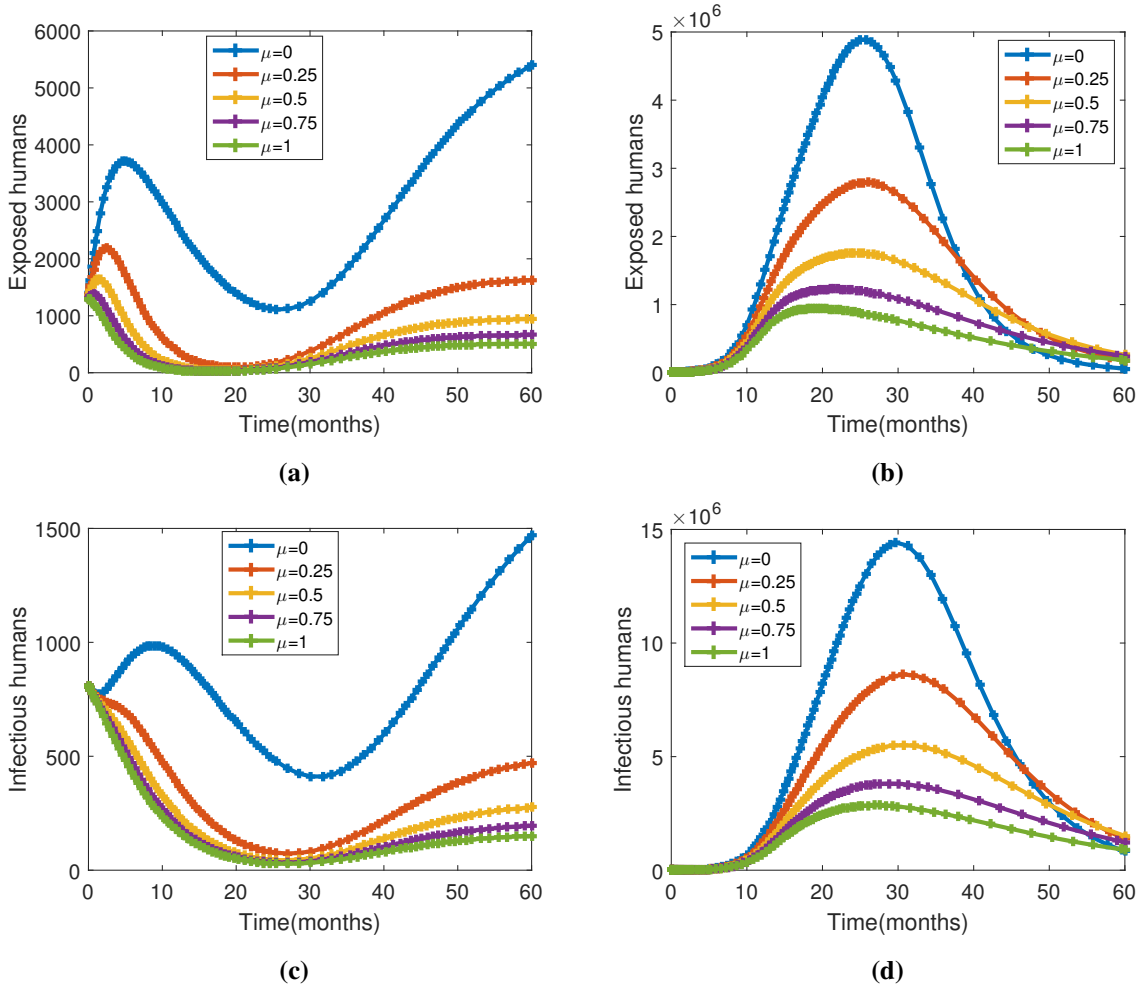

Figure 21. Figure demonstrating (**a**) the effect of post-exposure vaccination on exposed HUMs, varying post-exposure vaccination rate at $\mathcal{R}_c^h < 1$ and $\mathcal{R}_0^r < 1$, (**b**) the effect of post-exposure vaccination on exposed HUMs while $\mathcal{R}_c^h = 1.7981$ and $\mathcal{R}_0^r = 9.091$, when $\varrho_h = 0.9$, $\varpi = 0.000058$, and $p_h = 0.989$, (**c**) the effect of post-exposure vaccination on infectious HUMs, varying post-exposure vaccination rate at $\mathcal{R}_c^h < 1$ and $\mathcal{R}_0^r < 1$, and (**d**) the effect of post-exposure vaccination on infectious HUMs while $\mathcal{R}_c^h = 1.7981$ and $\mathcal{R}_0^r = 9.091$, when $\varrho_h = 0.9$, $\varpi = 0.000058$, and $p_h = 0.989$.

Figure 22a illustrates the impact of post-exposure vaccination on susceptible HUMs. When there is post-exposure vaccination in the HUM population, we noticed that when the post-vaccinate rate varies or increases, the susceptible HUMs increase over time. Also, it was noted that if the post-exposure vaccination against the disease is increased to almost perfect, the susceptible individuals grow over time. Figure 22b illustrates the impact of post-exposure vaccination on vaccinated HUMs. When there is post-exposure vaccination in the HUM population, we noticed that when the post-exposure vaccination rate varies or increases, the susceptible HUMs increases (that is, the population of vaccinated HUMs increases a little; note that $\mathcal{R}_c^h = 1.7981$ and $\mathcal{R}_0^r = 9.091$, when $\varrho_h = 0.9$, $\varpi = 0.000058$, and $p_h = 0.989$).

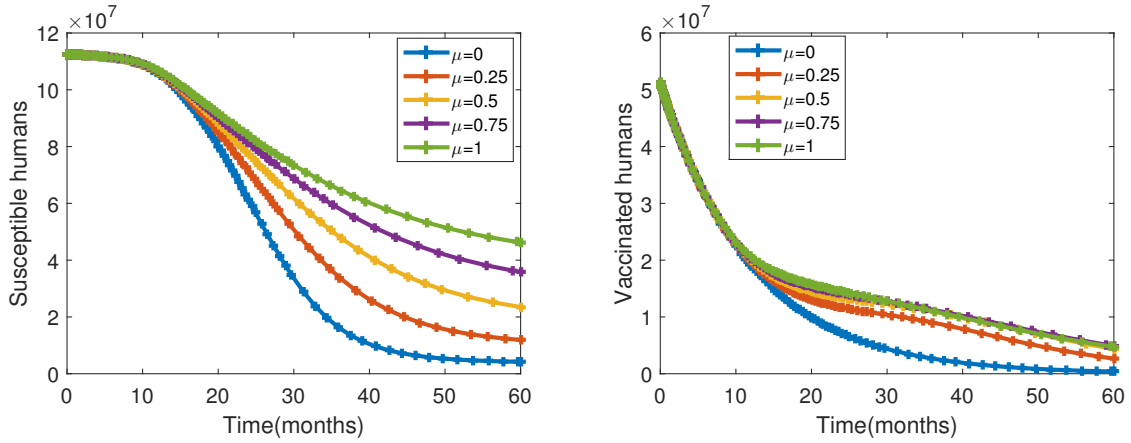

Figure 22. Figure demonstrating (**a**) the effect of post-exposure vaccination on susceptible HUMs, varying the post-exposure vaccination rate at $\mathcal{R}_c^h = 1.7981$ and $\mathcal{R}_0^r = 9.091$, when $\varrho_h = 0.9$, $\varpi = 0.000058$, and $p_h = 0.989$, and (**b**) the effect of post-exposure vaccination on vaccinated HUMs, varying the post-exposure vaccination rate at $\mathcal{R}_c^h = 1.7981$ and $\mathcal{R}_0^r = 9.091$, when $\varrho_h = 0.9$, $\varpi = 0.000058$, and $p_h = 0.989$.

Figure 23a illustrates the impact of early therapeutic education on exposed HUMs. When there is early therapeutic education in the HUM population, we noticed that when the early therapeutic education rate varies or increases, there is no effect (that is, the behaviour of the population of exposed HUMs remains unchanged; note that $\mathcal{R}_c^h < 1$ and $\mathcal{R}_0^r < 1$). Figure 23b illustrates the impact of early therapeutic education on exposed HUMs. When there is early therapeutic education control in the HUM population, we noticed that when the early therapeutic education rate varies or increases, the cases increases immensely around the 10–20th weeks and the cases reduce to a minimum after that (that is, the population of exposed HUMs reduces to zero or it wiped out the population from the environment; note that $\mathcal{R}_c^h = 1.7981$ and $\mathcal{R}_0^r = 9.091$, when $\varrho_h = 0.9$, $\varpi = 0.000058$, and $p_h = 0.989$). Figure 23c illustrates the impact of early therapeutic education on infectious HUMs. When there is early therapeutic education in the HUM population, we noticed that when the early therapeutic education rate varies or increases, it decreases around the 5–20th weeks, and the infectious HUMs increases after that, to some extent (that is, the population of exposed HUMs increases; note that $\mathcal{R}_c^h < 1$ and $\mathcal{R}_0^r < 1$). Figure 23d illustrates the impact of early therapeutic education on infectious HUMs. When there is early therapeutic education in the HUM population, we noticed that when the early therapeutic education rate varies or increases, the cases increase immensely around the 20–25th weeks and the cases reduce to a minimum after that (that is, the population of infectious HUMs reduces to minimum; note that $\mathcal{R}_c^h = 1.7981$ and $\mathcal{R}_0^r = 9.091$, when $\varrho_h = 0.9$, $\varpi = 0.000058$, and $p_h = 0.989$).

Figure 24a illustrates the impact of early therapeutic education on susceptible HUMs. When there is early therapeutic education in the HUM population, we observed that when the early therapeutic education rate varies or increases, the number of susceptible HUMs increases over time. Also, it was noted that if the early therapeutic education against the disease is increased to almost perfect, the susceptible individuals grow over time; note that $\mathcal{R}_c^h = 1.7981$ and $\mathcal{R}_0^r = 9.091$, when $\varrho_h = 0.9$, $\varpi = 0.000058$, and $p_h = 0.989$. Figure 24b illustrates the impact of early therapeutic education on

vaccinated HUMs. When there is early therapeutic education in the HUM population, we noticed that when the early therapeutic education rate varies or increases, the susceptible HUMs increases (that is, the population of vaccinated HUMs increases a little; note that $\mathcal{R}_c^h = 1.7981$ and $\mathcal{R}_0^r = 9.091$, when $\varrho_h = 0.9$, $\varpi = 0.000058$, and $p_h = 0.989$).

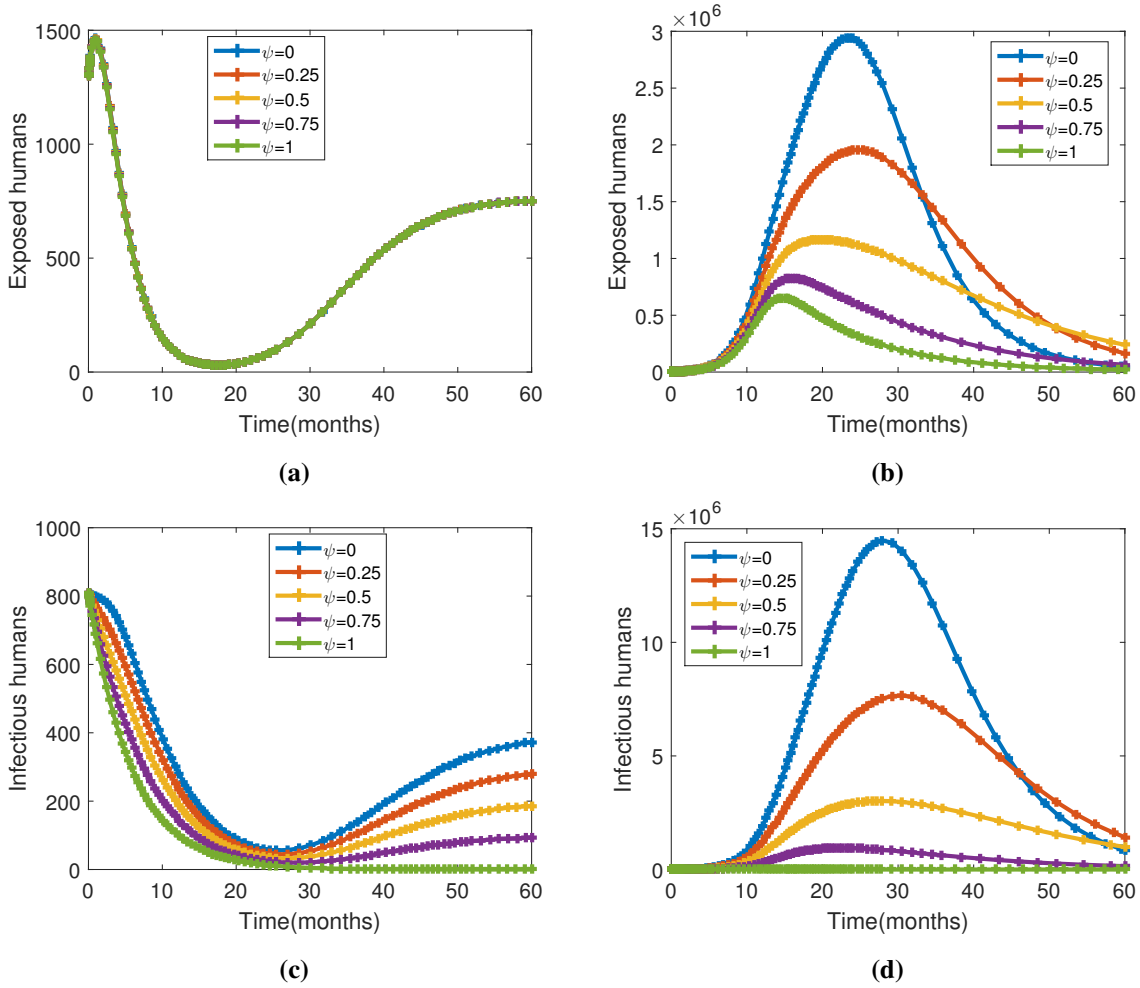

Figure 23. Figure demonstrating (**a**) the effect of early therapeutic education on exposed HUMs, varying early therapeutic education rate at $\mathcal{R}_c^h < 1$ and $\mathcal{R}_0^r < 1$, (**b**) the effect of early therapeutic education on exposed HUMs while $\mathcal{R}_c^h = 1.7981$ and $\mathcal{R}_0^r = 9.091$, when $\varrho_h = 0.9$, $\varpi = 0.000058$, and $p_h = 0.989$, (**c**) the effect of early therapeutic education on infectious HUMs while $\mathcal{R}_c^h = 1.7981$ and $\mathcal{R}_0^r = 9.091$, when $\varrho_h = 0.9$, $\varpi = 0.000058$, and $p_h = 0.989$, and (**d**) the effect of early therapeutic education on infectious HUMs, varying early therapeutic education rate at $\mathcal{R}_c^h < 1$ and $\mathcal{R}_0^r < 1$.

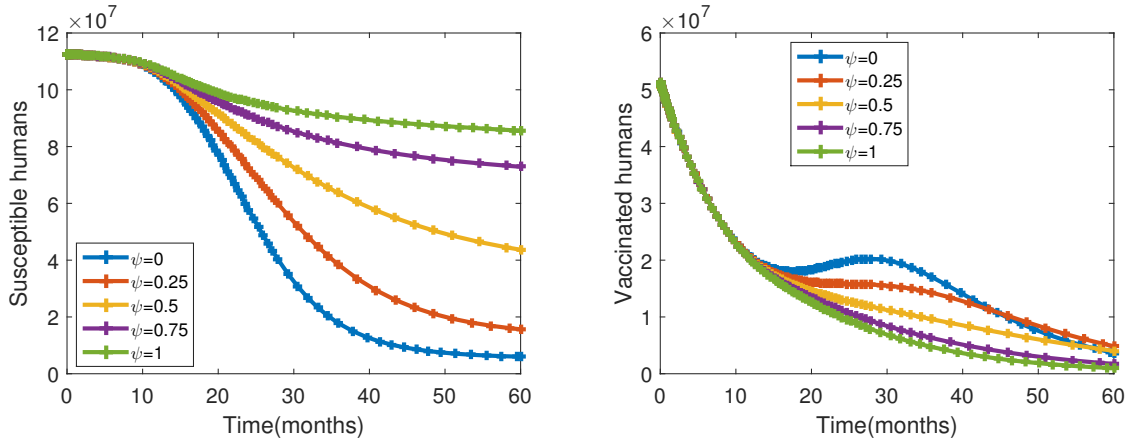

(a) **(b)**

Figure 24. Figure demonstrating (**a**) the effect of early therapeutic education on susceptible HUMs, varying the early therapeutic education rate at $\mathcal{R}_c^h = 1.7981$ and $\mathcal{R}_0^r = 9.091$, when $\varrho_h = 0.9$, $\varpi = 0.000058$, and $p_h = 0.989$, and (**b**) the effect of early therapeutic education on vaccinated HUMs, varying the early therapeutic education rate at $\mathcal{R}_c^h = 1.7981$ and $\mathcal{R}_0^r = 9.091$, when $\varrho_h = 0.9$, $\varpi = 0.000058$, and $p_h = 0.989$.

Figure 25a illustrates the impact of treatment on exposed HUMs. When there is treatment in the HUM population, we noticed that when the treatment rate varies or increases, there is an immense decrease in the population of exposed HUMs; note that $\mathcal{R}_c^h = 1.7981$ and $\mathcal{R}_0^r = 9.091$, when $\varrho_h = 0.9$, $\varpi = 0.000058$, and $p_h = 0.989$). Figure 25b illustrates the impact of treatment on infectious HUMs. When there is treatment control in the HUM population, we noticed that when the treatment rate varies or increases, the cases decrease immensely (that is, the population of infectious HUMs reduces to zero, or it wiped out the population of infectious HUMs from the environment; note that $\mathcal{R}_c^h = 1.7981$ and $\mathcal{R}_0^r = 9.091$, when $\varrho_h = 0.9$, $\varpi = 0.000058$, and $p_h = 0.989$). Figure 25c illustrates the impact of treatment on susceptible HUMs. When there is treatment in the HUM population, we noticed that when the treatment rate varies or increases, the susceptible HUMs increases over time. Also, it was noted that if the treatment against the disease is increased to almost perfect, the susceptible individuals grow over time; note that $\mathcal{R}_c^h = 1.7981$ and $\mathcal{R}_0^r = 9.091$, when $\varrho_h = 0.9$, $\varpi = 0.000058$, and $p_h = 0.989$. Figure 25d illustrates the impact of treatment on vaccinated HUMs. When there is treatment in the HUM population, we noticed that when the treatment rate varies or increases, the susceptible HUMs increases, (that is, the population of vaccinated HUMs increases a little; note that $\mathcal{R}_c^h = 1.7981$ and $\mathcal{R}_0^r = 9.091$ when $\varrho_h = 0.9$, $\varpi = 0.000058$, and $p_h = 0.989$).

Figure 26a illustrates the impact of imperfect vaccination on exposed HUMs. When vaccination is imperfect in the HUM population, we observed that as the vaccination rate varies or increases, the population of exposed HUMs decreases significantly. Note that $\mathcal{R}_c^h = 1.7981$ and $\mathcal{R}_0^r = 9.091$, when $\varrho_h = 0.9$, $\varpi = 0.000058$, and $p_h = 0.989$. Figure 26b illustrates the impact of imperfect vaccination on infectious HUMs. When there is imperfect vaccination control in the HUM population, we noticed that when the imperfect vaccination rate varies or increases, the cases decrease immensely (that is, the population of infectious HUMs reduces to zero, or it wiped out the population of infectious HUMs from the environment; note that $\mathcal{R}_c^h = 1.7981$ and $\mathcal{R}_0^r = 9.091$, when $\varrho_h = 0.9$, $\varpi = 0.000058$, and

$p_h = 0.989$). Figure 26c illustrates the impact of imperfect vaccination on vaccinated HUMs. When there is imperfect vaccination in the HUM population, we noticed that when the imperfect vaccination rate varies or increases, the susceptible HUMs increases, (that is, the population of vaccinated HUMs increases a little; note that $\mathcal{R}_c^h = 1.7981$ and $\mathcal{R}_0^r = 9.091$, when $\varrho_h = 0.9$, $\varpi = 0.000058$, and $p_h = 0.989$).

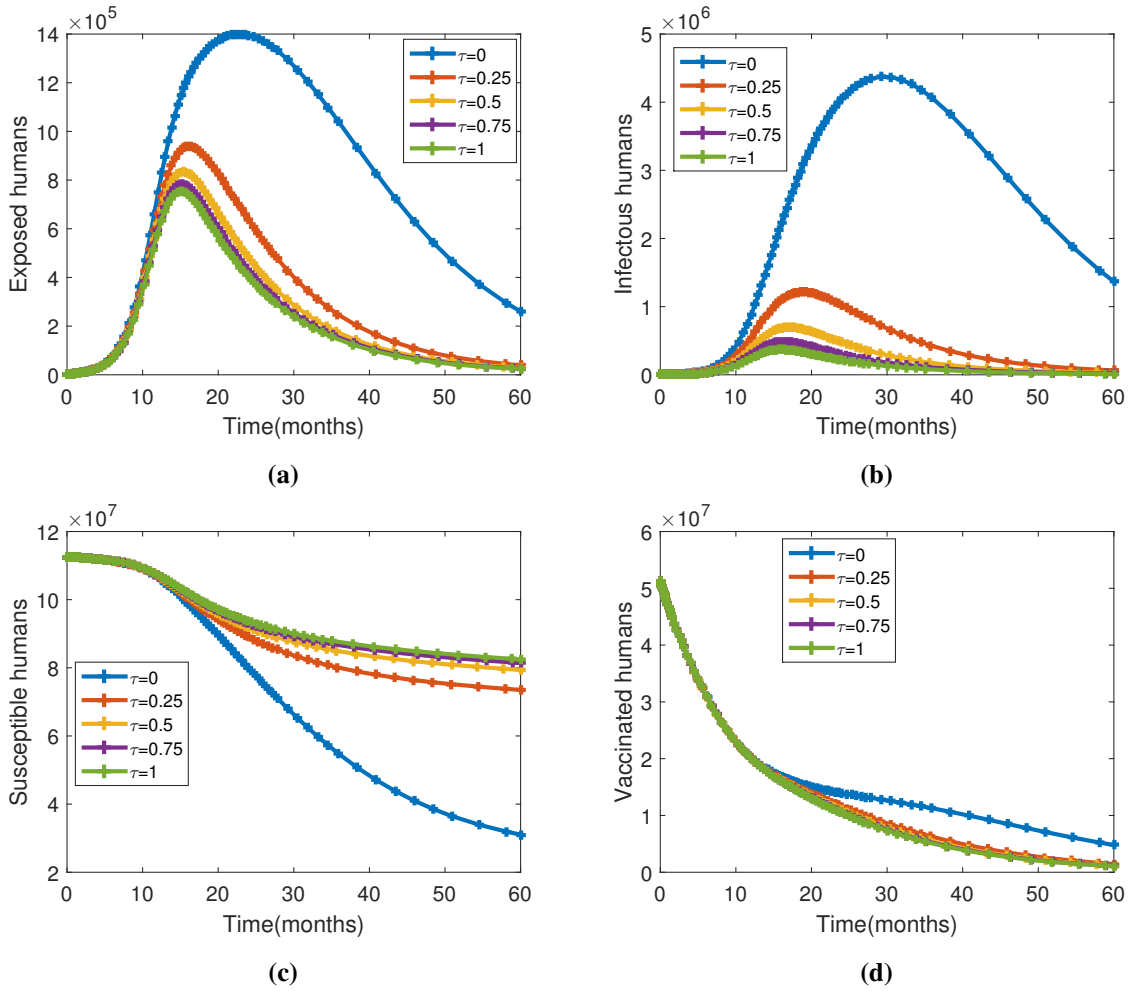

Figure 25. Figure demonstrating (**a**) the effect of treatment on exposed HUMs, varying treatment rate while $\mathcal{R}_c^h = 1.7981$ and $\mathcal{R}_0^r = 9.091$, when $\varrho_h = 0.9$, $\varpi = 0.000058$, and $p_h = 0.989$, (**b**) the effect of treatment on exposed HUMs, varying treatment rate while $\mathcal{R}_c^h = 1.7981$ and $\mathcal{R}_0^r = 9.091$, when $\varrho_h = 0.9$, $\varpi = 0.000058$, and $p_h = 0.989$, (**c**) the effect of treatment on infectious HUMs, varying treatment rate while $\mathcal{R}_c^h = 1.7981$ and $\mathcal{R}_0^r = 9.091$, when $\varrho_h = 0.9$, $\varpi = 0.000058$, and $p_h = 0.989$, and (**d**) the effect of treatment on infectious HUMs, varying treatment rate while $\mathcal{R}_c^h = 1.7981$ and $\mathcal{R}_0^r = 9.091$, when $\varrho_h = 0.9$, $\varpi = 0.000058$, and $p_h = 0.989$.

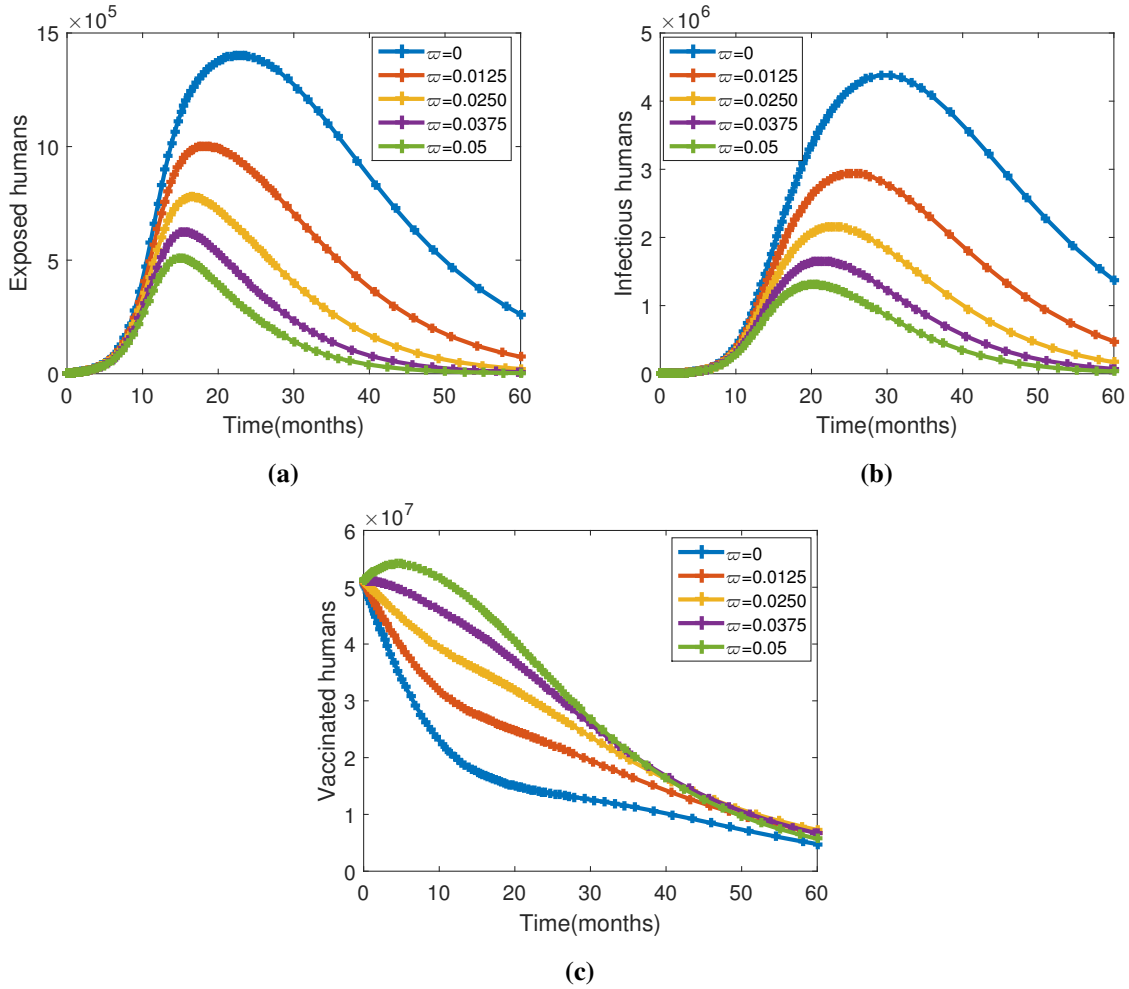

Figure 26. Figure demonstrating (**a**) the effect of imperfect vaccination on exposed HUMs, varying imperfect vaccination rate while $\mathcal{R}_c^h = 1.7981$ and $\mathcal{R}_0^r = 9.091$, when $\varrho_h = 0.9$, $\varpi = 0.000058$, and $p_h = 0.989$, (**b**) the effect of imperfect vaccination on exposed HUMs, varying imperfect vaccination rate while $\mathcal{R}_c^h = 1.7981$ and $\mathcal{R}_0^r = 9.091$, when $\varrho_h = 0.9$, $\varpi = 0.000058$, and $p_h = 0.989$, and (**c**) The effect of imperfect vaccination on infectious HUMs, varying imperfect vaccination rate while $\mathcal{R}_c^h = 1.7981$ and $\mathcal{R}_0^r = 9.091$, when $\varrho_h = 0.9$, $\varpi = 0.000058$, and $p_h = 0.989$.

Figure 27a illustrates the impact of imperfect vaccination on susceptible HUMs. When vaccination is imperfect in the HUM population, we observed that as the vaccination rate varies or increases, the number of susceptible HUMs decreases over time. Also, it was noted that if imperfect vaccination against the disease is increased to almost perfect, the susceptible individuals' population drops over time. Note that $\mathcal{R}_c^h = 1.7981$ and $\mathcal{R}_0^r = 9.091$, when $\varrho_h = 0.9$, $\varpi = 0.000058$, and $p_h = 0.989$. Figure 27b illustrates the impact of imperfect vaccination on vaccinated HUMs. When there is imperfect vaccination in the HUM population, we noticed that when the imperfect vaccination rate varies or increases, the susceptible HUMs increase, (that is, the population of vaccinated HUMs increases a little; note that $\mathcal{R}_c^h = 1.7981$ and $\mathcal{R}_0^r = 9.091$, when $\varrho_h = 0.9$, $\varpi = 0.000058$, and $p_h = 0.989$).

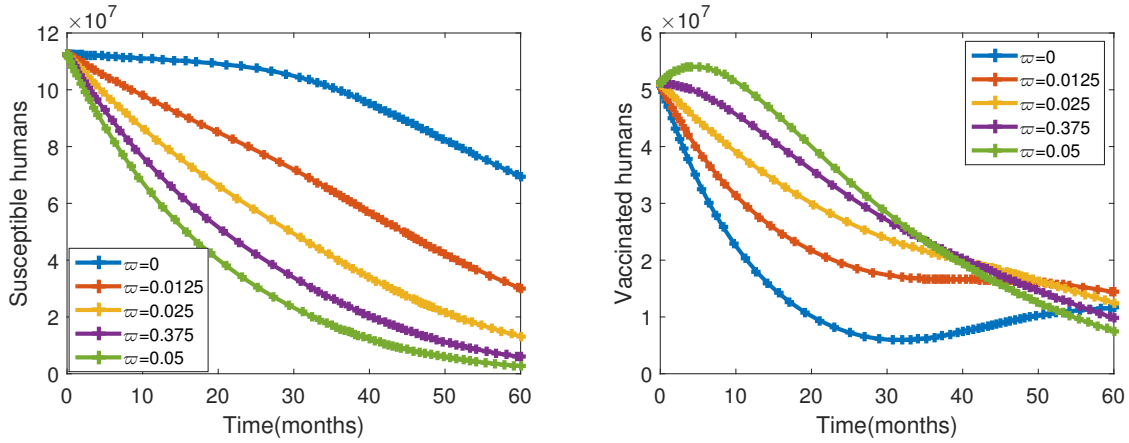

(a) **(b)**

Figure 27. Figure demonstrating (**a**) the effect of imperfect vaccination on susceptible HUMs, varying the imperfect vaccination education rate when $\mathcal{R}_c^h < 1$ and $\mathcal{R}_0^r < 1$, and (**b**) the effect of imperfect vaccination on vaccinated HUMs, varying the imperfect vaccination rate at $\mathcal{R}_c^h < 1$ and $\mathcal{R}_0^r < 1$.

5.2. Seasonal dynamics simulation of the model equation

Our models' understanding of transmission dynamics is enhanced by including seasonal variation. This strategy provides decision-makers with possible outbreak dates, enabling more efficient resource use and focused efforts to reduce the burden of disease. However, the majority of MDs for Mpox frequently ignore these aspects. Full application of this strategy in our model is constrained by the unavailability of primary data; thus, we rely on scarce secondary data. Climate-dependent variations in rodent abundance, especially rainfall, which affects breeding sites, affect seasonal patterns of diseases caused by rodents such as Mpox. To better represent transmission patterns, we update our model equation (2.1) by incorporating seasonality into vector dynamics. Using time-dependent functions, we concentrate on altering the rodent recruitment rate (Φ_r) and constant transmission rate (ϱ_r). The following is the definition of the time-dependent transmission rate, $\varrho_r(t)$:

$$\varrho_r(t) = \varrho_r(0)\left(1 + \rho cos\left(\frac{2\pi t}{T} + \theta\right)\right). \tag{5.1}$$

Taking into account seasonal breeding by making the rodents recruitment rate (Φ_r) dependent on rainfall, as follows:

$$\Phi_r(t) = \Phi_r(0)(1 + \kappa \times \mathbf{rainfall}(t)). \tag{5.2}$$

Where

- ρ is the amplitude of seasonal fluctuation,
- T is a period (usually 365 for annual cycle),
- θ is a phase shift (to align with seasonal peaks),
- $\varrho_r(0)$ is the transmission rate of rodent to rodent,
- $\Phi_r(0)$ is a rodent recruitment rate,
- κ is a rainfall-to-breeding efficiency coefficient,

- **Rainfall model**: use satellite data (CHIRPS) with logistic, growth:

$$\textbf{Rainfall}(t) = \frac{R_{max}}{1 + e^{-k(t-t_{peak})}}, \tag{5.3}$$

- R_{max} is a maximum monthly rainfall,
- t_{peak} is a timing of peak rainfall,
- k is a rate of growth.

Justification biologically: In infectious disease modeling, the cosine-based periodic function is frequently used to depict seasonally fluctuating transmission pathways. Variations in human social behavior, mobility patterns, and contact intensity are the main drivers of seasonal impacts on Mpox. These variations can be influenced by cultural events, school calendars, occupational activities, and weather. Additionally, because of changes in immunological function, co-circulating infections, and nutritional conditions, seasonal variation may indirectly affect host susceptibility. The strength of seasonal modulation is measured by the parameter ϵ. Greater values of ϵ indicate more seasonal impacts, while $\epsilon = 0$ reduces the model to a non-seasonal framework. This formulation permits analytical and numerical comparison between seasonal and non-seasonal circumstances, guarantees mathematical smoothness, and maintains the positivity of solutions. The model can capture repeated waves of Mpox transmission and evaluate the effectiveness of early therapeutic education and control methods under realistic, time-varying epidemiological conditions by incorporating seasonal forcing.

Figures 28–31 reveal a strong association between rainfall intensity and the population dynamics of susceptible, exposed, and infected rodents. The synthetic rainfall pattern (Figure 28) exhibits clear periodic fluctuations that serve as a major environmental driver influencing rodent population behavior. As shown in the susceptible rodent plot (Figure 29), increases in rainfall create favorable ecological conditions, leading to a rise in the susceptible population due to improved food availability and habitat conditions. This rise is followed by an increase in the number of exposed rodents (Figure 30), as higher rodent density and environmental moisture increase the likelihood of contact with infectious agents. Subsequently, the infected rodent population (Figure 31) also exhibits cyclical peaks that closely follow rainfall patterns, reflecting the influence of rainfall on disease transmission and persistence within the rodent population. The synchronized oscillations across all plots demonstrate that rainfall-induced seasonality plays a critical role in shaping the epidemiological dynamics of rodent-borne infections, linking environmental variability directly to fluctuations in rodent susceptibility, exposure, and infection levels.

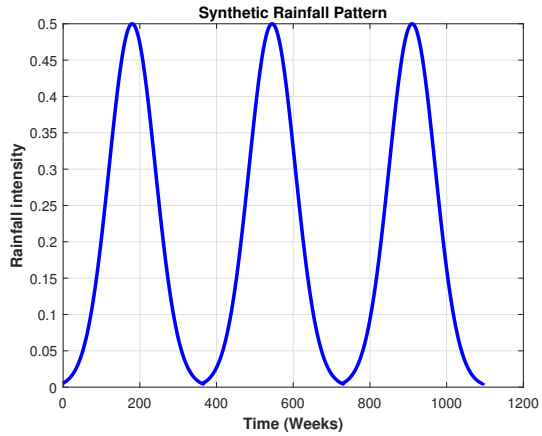

Figure 28. Synthetic rainfall pattern illustrating periodic climatic variation that affects rodent populations.

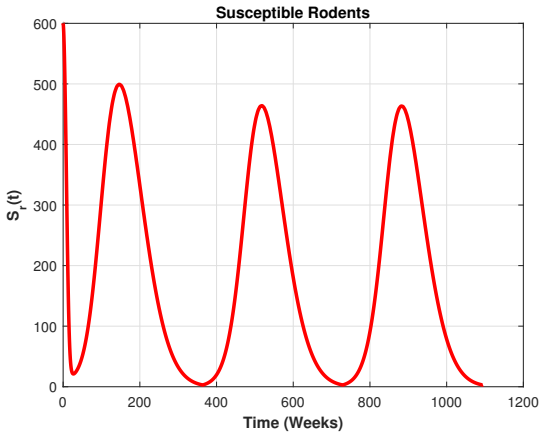

Figure 29. Variation in susceptible rodents reflecting the impact of rainfall on population growth and infection risk.

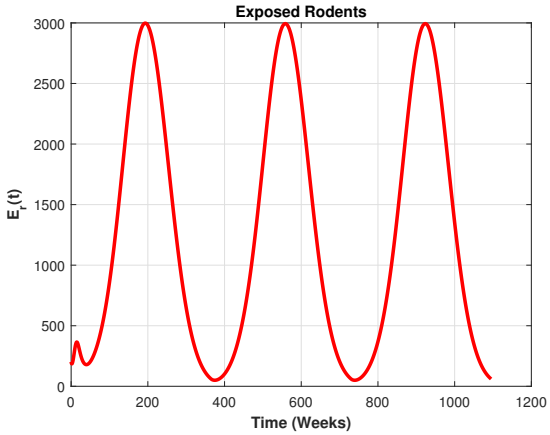

Figure 30. Temporal dynamics of exposed rodents showing periodic increases influenced by rainfall intensity.

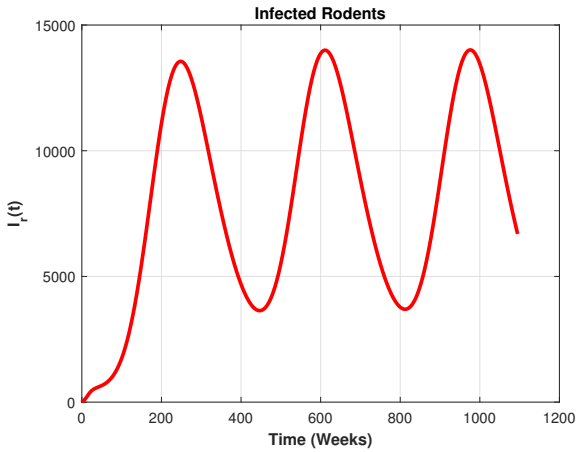

Figure 31. Cyclical pattern of infected rodents indicating rainfall-driven fluctuations in disease transmission.

6. Conclusions and recommendations

In this work, we formulated an MD of Mpox to assess the impact of early therapeutic education on seasonal variation. In the formulation, we considered early therapeutic education, imperfect vaccination, and post-exposure vaccination. We investigated the existence of backward bifurcation and found that an imperfect vaccination rate can trigger it in the Mpox dynamics. Data fitting has been performed using Nigerian data from May 2022 to May 2023. We proved that our model is fit to study Mpox virus, since our model is well-fitted. In the sensitivity analysis subsection, we have seen that early therapeutic education is the most sensitive parameter for controlling Mpox in the HUM population, since it affects the HUM control reproduction number the most, followed by imperfect vaccination. Furthermore, we have noticed that the contact effectiveness rates of HUMs are the most sensitive parameter in increasing the spread of Mpox in the environment, followed by the HUM natural death rate. In the numerical analysis simulation section, we noticed that education helps reduce the number of Mpox cases in the HUM population. The imperfect vaccination also helps, to some extent, in bringing down case numbers. Additionally, we noticed that post-exposure vaccination can reduce Mpox cases. We also assessed the impact of treatment on Mpox dynamics. We found that treatment also helps significantly reduce the number of cases. Finally, we assessed the impact of the early therapeutic education rate on Mpox dynamics. We found that the early therapeutic education approach is the best way to tackle the re-emergence of Mpox in the HUM population.

Finally, we recommend improving the current imperfect vaccination to effectively prevent future re-emergence of the disease in the HUM population. We also suggest using an early therapeutic education approach to control the re-emergence of Mpox disease in the HUM population.

6.1. Comparative efficacy of control techniques and policy-relevant insights

Compared with other interventions at similar intensity levels, our findings show that early therapeutic education produces the greatest reduction in the infectious human population over time. In particular, raising the early therapeutic education rate (ψ) outperforms increases in vaccination coverage or treatment rate alone in reducing the peak and cumulative number of infected individuals.

Quantitatively, compared to comparable relative increases in the vaccine rate (ϖ) or treatment rate (τ), a small increase in ψ results in a greater proportionate decrease in infection prevalence.

From an epidemiological perspective, early therapeutic education prevents the spread of the disease by acting at the exposed stage. Its superior performance compared to therapies that intervene later in the illness cycle, such as treating infectious individuals, can be explained by this preventive mechanism. Additionally, by reducing the number of secondary infections produced during peak transmission periods, especially under seasonal forcing, early therapeutic education indirectly lowers the effective reproduction number. From a policy standpoint, these results imply that early therapeutic education is an affordable and quickly implementable intervention, particularly in places with limited resources where vaccination availability and healthcare infrastructure may be limited. Even in the presence of seasonal variations, Mpox transmission can be significantly reduced through educational programs that encourage early symptom recognition, prompt healthcare-seeking, and adherence to preventive treatments. Overall, the model shows that the largest epidemiological effect is obtained by integrating early therapeutic education with immunization and treatment measures. However, early therapeutic education turns out to be the most effective single control tool for lowering Mpox transmission and minimizing epidemic recurrence when interventions are prioritized separately.

Author contributions

Mohammed M Al-Shomrani: Formalization, Investigation, Supervision, Visualization, Validation; Abdullahi Yusuf: Writing the original draft, Methodology, Conceptualization.

Use of Generative-AI tools declaration

The authors declare they have not used Artificial Intelligence (AI) tools in the creation of this article.

Funding

This project was funded by the Deanship of Scientific Research (DSR) at King Abdulaziz University, Jeddah, Saudi Arabia, under grant No. (IPP: 360-130-2025). The authors therefore acknowledge DSR with thanks for its technical and financial support.

Data availability statement

All data used in this work are presented within the manuscript.

Conflicts of interest

There is no competing interest whatsoever in this paper.

References

1. Md. A. I. Islam, M. H. M. Mubassir, A. K. Paul, S. S. Shanta, A mathematical model for understanding and controlling Mpox transmission dynamics in the USA and its implications for future epidemic management, *Decoding Infection and Transmission*, **2** (2024), 100031. https://doi.org/10.1016/j.dcit.2024.100031
2. J. Kongson, C. Thaiprayoon, W. Sudsutad, Analysis of a mathematical model for the spreading of the Mpox virus with a constant proportional-Caputo derivative operator, *AIMS Mathematics*, **10** (2025), 4000–4039. https://doi.org/10.3934/math.2025187
3. S. Anil, B. Joseph, M. Thomas, V. K. Sweety, N. Suresh, T. Waltimo, Monkeypox: a viral zoonotic disease of rising global concern, *Infectious Diseases & Immunity*, **4** (2024), 121–131. https://doi.org/10.1097/ID9.0000000000000124
4. J. Molla, I. Sekkak, A. M. Ortiz, I. Moyles, B. Nasri, Mathematical modeling of Mpox: a scoping review, *One Health*, **16** (2023), 100540, https://doi.org/10.1016/j.onehlt.2023.100540
5. E. M. Bunge, B. Hoet, L. Chen, F. Lienert, H. Weidenthaler, L. R. Baer, et al., The changing epidemiology of human Mpox—A potential threat? A systematic review, *PLoS Negl. Trop. Dis.*, **16** (2022), e0010141. https://doi.org/10.1371/journal.pntd.0010141
6. Centres for Disease Control and Prevention, About Monkeypox, 2023. Available from: `https://www.cdc.gov/monkeypox/about/index.html`.
7. S. T. Rehan, H. U. Hussain, K. A. Kumar, M. Sukaina, Z. Khan, A. J. Nashwan, Global Mpox virus outbreak 2022: a bibliometric analysis, *Cureus*, **15** (2023), e37107. https://doi.org/10.7759/cureus.37107
8. World Health Organization, Mpox (Mpox) outbreak 2022-Global, 2022. Available from: `https://www.who.int/emergencies/situations/monkeypox-oubreak-2022/1000`.
9. A. W. Rimoin, N. Kisalu, B. Kebela-Ilunga, T. Mukaba, L. L. Wright, P. Formenty, et al., Endemic human monkey pox, Democratic Republic of Congo, 2001–2004, *Emerg. Infect. Dis.*, **13** (2007), 934–937. https://doi.org/10.3201/eid1306.061540
10. Centers for Disease Control and Prevention, Morbidity and Mortality Weekly Report, Volume 52, November 7, 2003, No. 44. Available from: `https://stacks.cdc.gov/view/cdc/28471/cdc_28471_DS1.pdf`.
11. O. I. Idisi, T. T. Yusuf, E. Adeniyi, A. A. Onifade, Y. T. Oyebo, A. T. Samuel, et al., A new compartmentalized epidemic model to analytically study the impact of awareness on the control and mitigation of the monkeypox disease, *Healthcare Analytics*, **4** (2023), 100267. https://doi.org/10.1016/j.health.2023.100267
12. B. Cabanillas, G. Murdaca, A. Guemari, M. J. Torres, A. K. Azkur, E. Aksoy, et al., Mpox 2024 outbreak: fifty essential questions and answers, *Allergy*, **79** (2024), 3285–3309. https://doi.org/10.1111/all.16374
13. D. N. Tanko, F. A. Abdullah, M. K. M. Ali, M. O. Adewole, J. Andrawus, Analyzing onchocerciasis transmission dynamics through mathematical models incorporating early therapeutic intervention and vector control, *IAENG International Journal of Applied Mathematics*, **55** (2025), 3579–3599.

14. D. N. Tanko, F. A. Abdullah, M. K. M. Ali, M. O. Adewole, J. Andrawus, Onchocerciasis control dynamics: a focus on early treatment and vector management strategies, *Journal of the Nigerian Society of Physical Sciences*, **8** (2026), 2942. https://doi.org/10.46481/jnsps.2026.2942

15. O. J. Peter, S. Kumar, N. Kumari, F. A. Oguntolu, K. Oshinubi, R. Musa, Transmission dynamics of Mpox virus: a mathematical modelling approach, *Model. Earth Syst. Environ.*, **8** (2022), 3423–3434. https://doi.org/10.1007/s40808-021-01313-2

16. B. Liu, S. Farid, S. Ullah, M. Altanji, R. Nawaz, S. W. Teklu, Mathematical assessment of Mpox disease with the impact of vaccination using a epidemiological modeling approach, *Sci. Rep.*, **13** (2023), 13550. https://doi.org/10.1038/s41598-023-40745-x

17. M. I. Betti, L. Farrell, J. Heffernan, A pair formation model with recovery: application to Mpox, *Epidemics*, **44** (2023), 100693. https://doi.org/10.1016/j.epidem.2023.100693

18. T. D. Alharbi, M. R. Hasan, Modeling Mpox dynamics with human–rodent interactions and waning vaccination, *AIMS Math.*, **10** (2025), 18660–18679. https://doi.org/10.3934/math.2025834

19. H. Iftikhar, M. Daniyal, M. Qureshi, K. Tawaiah, R. K. Ansah, J. K. Afriyie, A hybrid forecasting technique for infection and death from the Mpox virus, *Digit. Health*, **9** (2023), 1–17. https://doi.org/10.1177/20552076231204748

20. A. Elsonbaty, W. Adel, A. Aldurayhim, A. El-Mesady, Mathematical modeling and analysis of a novel monkeypox virus spread integrating imperfect vaccination and nonlinear incidence rates, *Ain Shams Eng. J.*, **15** (2024), 102451. https://doi.org/10.1016/j.asej.2023.102451

21. Y. Yang, C. Li, X. Fan, W. Long, Y. Hu, Y. Wang, et al., Effectiveness of omadacycline in a patient with chlamydia psittaci and KPC-producing gram-negative bacteria infection, *Infect. Drug Resist.*, **18** (2025), 903–908. https://doi.org/10.2147/IDR.S505311

22. Y. Wang, Q. Wang, T. W. Yang, J. M. Yin, F. Wei, H. Liu, et al., Analysis of immune and inflammatory microenvironment characteristics of noncancer end-stage liver disease, *J. Interf. Cytok. Res.*, **43** (2023), 86–97. https://doi.org/10.1089/jir.2022.0172

23. L. Tang, Y. Chen, Q. Xiang, J. Xiang, Y. Tang, J. Li, The association between IL18, FOXP3 and IL13 genes polymorphisms and risk of allergic rhinitis: a meta-analysis, *Inflamm. Res.*, **69** (2020), 911–923. https://doi.org/10.1007/s00011-020-01368-4

24. N. Ndembi, P. Mbala-Kingebeni, B. Khalifa, M. L. Mazaba, M. O. Foláyan, Are there ecological and seasonal factors influencing the resurgence of Mpox in Africa?, *J. Public Health Afr.*, **15** (2024), a823. https://doi.org/10.4102/jphia.v15i1.823

25. M. Karuhanga, V. Yiga, A mathematical model for the dynamics of onchocerciasis with vector control and mass disease administration, *J. Appl. Math.*, **2024** (2024), 6683371. https://doi.org/10.1155/2024/6683371

26. U. E. Michael, L. O. Omenyi, E. Kafayat, E. Nwaeze, O. A. Akachukwu, G. Ozoigbo, et al., Monkeypox mathematical model with surveillance as control, *Commun. Math. Biol. Neurosci.*, **2023** (2023), 6.

27. S. Wang, K. Zhang, A. Liu, Flat-Lattice-CNN: a model for Chinese medical-named-entity recognition, *PLoS One*, **20** (2025), e0331464. https://doi.org/10.1371/journal.pone.0331464

28. W. Wang, J.-X. Li, S.-Q. Long, Z.-N. Liu, X.-P. Li, Z.-H. Peng, et al., Emerging strategies for monkeypox: antigen and antibody applications in diagnostics, vaccines, and treatments, *Military Med. Res.*, **12** (2025), 69. https://doi.org/10.1186/s40779-025-00660-w

29. J. Andrawus, Y. U. Ahmad, A. A. Andrew, A. Yusuf, S. Qureshe, B. A. Denue, et al., Impact of surveillance in human-to-human transmission of Mpox virus, *Eur. Phys. J. Spec. Top.*, **234** (2024), 483–514. https://doi.org/10.1140/epjs/s11734-024-01346-5

30. Y. U. Ahmad, J. Andrawus, A. Ado, Y. A. Maigoro, A. Yusuf, S. Althobaiti, et al., Mathematical modeling and analysis of human-to-human Mpox virus transmission with post-exposure vaccination, *Model. Earth Syst. Environ.*, **10** (2024), 2711–2731. https://doi.org/10.1007/s40808-023-01920-1

31. G. D. Yaleu, S. Bowong, E. H. Danga, J. Kurths, Mathematical analysis of the dynamical transmission of Neisseria meningitidis serogroup A, *Int. J. Comput. Math.*, **94** (2017), 2409–2434. http://doi.org/10.1080/00207160.2017.1283411

32. O. Diekmann, J. A. P. Heesterbeek, J. A. J. Metz, On the definition and the computation of the basic reproduction ratio $\mathcal{R}_c$ in models for infectious diseases in heterogeneous populations, *J. Math. Biol.*, **28** (1990), 365–382. https://doi.org/10.1007/BF00178324

33. P. Van De Driessche, J. Watmough, Reproduction number sub-threshold Endemic Equilibrium for compartmental models of disease transmission, *Math. Biosci.*, **180** (2002), 29–48. https://doi.org/10.1016/S0025-5564(02)00108-6

34. J. Andrawus, S. Abdulrahman, R. V. K. Singh, S. S. Manga, Sensitivity analysis of mathematical modeling of Ebola virus population dynamics in the presence of vaccine, *Dutse Journal of Pure and Applied Sciences*, **8** (2022), 40–46. https://doi.org/10.4314/dujopas.v8i2a.5

35. J. Andrawus, A. Yusuf, U. T. Mustapha, A. S. Alshomrani, D. Baleanu, Unravelling the dynamics of Ebola virus with contact tracing as control strategy, *Fractals*, **31** (2023), 2340159. https://doi.org/10.1142/S0218348X2340159X

36. C. Castillo-Chavez, B. Song, Dynamical models of tuberculosis and their applications, *Mathematical Biosciences and Engineering*, **1** (2004), 361–404. https://doi.org/10.3934/mbe.2004.1.361

37. C. Castillo-Chavez, Z. Feng, W. Huang, On the computation of R_0 and its role on global stability, In: *Mathematical approaches for emerging and reemerging infectious diseases: an introduction*, New York: Springer, 2002, 229–250.

38. C. Castillo-Charvez, B. Song, Dynamical model of tuberculosis and their applications, *Mathematical Biosciences and Engineering*, **1** (2004), 361–404. https://doi.org/10.3934/mbe.2004.1.361

39. F. Y. Eguda, J. Andrawus, S. Babuba, The solution of a mathematical model for Dengue fever transmission using the differential method, *Journal of the Nigerian Society of Physical Sciences*, **1** (2019), 82–87. https://doi.org/10.46481/jnsps.2019.18

40. J. P. La Salle, *The stability of dynamical systems*, Philadelphia: SIAM, 1976. https://doi.org/10.1137/1.9781611970432

41. J. Andrawus, E. Y. Felix, Mathematical analysis of a model for syphilis endemicity, *International Journal of Scientific Engineering and Applied Science*, **3** (2017), 48–72.

AIMS Press